

**MOLECULAR DYNAMICS SIMULATIONS TO DEVELOP NOVEL  
SOLVENTS FOR DEEP DESULFURIZATION OF DIESEL**

**Dinara Gapeyenko, Bachelor in Chemical Engineering**

**Submitted in fulfilment of the requirements for the degree of Master of  
Science in Chemical Engineering**



**School of Engineering**

**Department of Chemical Engineering**

**Nazarbayev University**


**53 KABANBAY BATYR AVENUE,  
ASTANA, KAZAKHSTAN, 010000**

**Supervisors: Dhawal Shah & Mehdi Torkmahalleh**

**December 2017**

## DECLARATION

I hereby, declare that this manuscript, entitled “Molecular dynamics simulations to develop novel solvents for deep desulfurization of diesel”, is the result of my own work except for quotations and citations which have been duly acknowledged. I also declare that, to the best of my knowledge and belief, it has not been previously or concurrently submitted, in whole or in part, for any other degree or diploma at Nazarbayev University or any other national or international institution.

(signature of author)  \_\_\_\_\_

Name: Dinara Gapeyenko

Date: 14.12.2017

# Abstract

For the last decade, deep eutectic solvent (DES), a novel solvent, has gathered lots of attention due to their favorable properties such as a low melting point, non-toxicity and low-cost. In this work, a combination of tetrabutylammonium chloride (TBAC), polyethylene glycol (PEG-200), and ferric chloride ( $\text{FeCl}_3$ ) at a molar ratio of 4:1:0.05, a metallic based deep eutectic solvent is analyzed using molecular dynamics simulation. The analysis reveals the interactions between the components of DES, which might lead to the formation of the DES, i.e., strong depression in the melting point as compared to the individual component. Further, the solvent was also tested for fuel desulfurization using molecular simulations. For the analysis n-octane was chosen as fuel with ~2000 ppm dibenzothiophene and the results suggest strong absorption of sulfur compounds by the DES. Molecular dynamics simulations were performed using GROMACS to explore different interactions occurring between the components of the DESs and model oil at a molecular level. Interaction energies between compounds and radial distribution functions indicate a strong interaction between the tetrabutylammonium ion with the dibenzothiophene molecule. The given work also shows that the DES can be applied for diesel even with high initial concentration of sulfur content and can be applicable for extraction of different sulfur compounds such as benzothiophene (BT) and thiophene (TS). Additionally, among all tested temperature ranges it was found that use of the room

temperature is beneficial for the desulfurization process. Moreover, composition of DES was varied by selectively removing either PEG or  $\text{FeCl}_3$  from the DES to evaluate the influence of each compound on the efficiency of desulfurization process.

# Acknowledgements

First of all, I want to thank my supervisor Dr. Dhawal Shah for giving me invaluable knowledge and constant support: understanding, patience and readiness to help me anytime. Also, I want to thank my alma mater Nazarbayev University who gave me opportunity to study at the MSc program, access to all its facilities and financial support to participate in the International conference “PHENMA-2017” which was held in Jabalpur, India on 14-16<sup>th</sup> of October 2017. And last, but not the least, I am very grateful for my family and friends who believed in me and gave me moral support whenever I needed it.

# Contents

<b>Abstract</b> .....	ii
<b>Acknowledgements</b> .....	iv
<b>List of figures</b> .....	vi
<b>Table of contents</b> .....	v
<b>List of tables</b> .....	vii
<b>Chapter 1 - Introduction</b> .....	1
1.1 Objective .....	3
<b>Chapter 2 – DESs and their applications in desulfurization</b> .....	5
2.1 Deep eutectic solvents.....	5
2.2. Formation of DES. ....	7
2.3 Application.....	9
2.3.1 Metal processing. ....	10
2.3.2 Organic synthesis application .....	11
2.3.3 Gas adsorption .....	13
2.3.4 Oil and gas industry .....	14
<b>Chapter 3 - Simulation methodology</b> .....	26
3.1 Molecular dynamics simulation.....	26
3.2 GROMACS TOOL .....	28
3.3 Systems simulated.....	31
3.4 Force validation. ....	34
<b>Chapter 4 - Results and discussion</b> .....	37
4.1 DES formation .....	37
4.2 Desulfurization process.....	39
4.3 Effect of process parameters on extraction process. ....	43
4.3.1 Concentration of the thiophenic compounds .....	43
4.3.2 Effect of temperature on the extraction process. ....	46
4.3.3 Varying the type of thiophenes .....	47
4.4 Effect of DES constituent on the extraction process .....	50
4.4.1 TBAC:PEG .....	50
4.4.2 TBAC:FeCl <sub>3</sub> .....	52
<b>Chapter 5 - Conclusion and future work</b> .....	55
<b>Reference list</b> .....	57
<b>Appendix</b> .....	60

# List of figures

Figure 1.1. Formation of eutectic point in a phase diagram. ....	3
Figure 2.1. Use of $\text{ChCl}/\text{urea}$ in organic reactions.....	12
Figure 2.2. Selective N-alkylation of aromatic amines.....	112
Figure 2.3. Reaction between epoxide with $\text{CO}_2$ in the DES. ....	14
Figure 2.4. MDESs and their efficiencies. ....	20
Figure 2.5. Molar ratio for DES.....	20
Figure 2.6. Effect of temperature on the efficiency. ....	20
Figure 2.7. Effect of mass ratio on the efficiency. ....	20
Figure 2.8. Effect of mixing speed on the efficiency.....	20
Figure 2.9. Effect of sulfur concentration on the efficiency. ....	20
Figure 2.10. DBT removal by different DESs (1g) for 10 minutes from model oil (5 mL). ....	23
Figure 2.11. Different sulfur compounds removal by $[\text{C}_{12}\text{DMEA}]\text{Cl}/\text{FeCl}_3$ .....	23
Figure 3.1. Simulation worksheet for the Thiophene compound.....	30
Figure 3.2. Simulated box of 500 thiophene molecules through VMD tool.....	34
Figure 3.3. Density of TS over temperature.....	35
Figure 4.1. Radial distribution functions between the TBA ion and Cl ion for system I and II..	37
Figure 4.2. Radial distribution function between the TBA ion and PEG system.....	37
Figure 4.3. Interaction energy profile for TBAC and DES systems.....	39
Figure 4.4. Interaction energy profile for DBT-octane and DBT-DES system.....	40
Figure 4.5 Interaction energies for DES compounds with DBT.....	41
Figure 4.6. Rdfs for DBT with octane,PEG and TBA inside the system 4. ....	42
Figure 4.7. DBT molecule surrounded by octane (black).....	43
Figure 4.8. DBT molecule captured by DES (red).....	43
Figure 4.9. The summary of interaction energies for different systems.....	44
Figure 4.10. Rdfs for DBT with octane, TBA and PEG for the system 7.....	45
Figure 4.11. Rdfs for DBT with octane, TBAC and PEG at the system 8.....	46
Figure 4.12. The extraction efficiency for sulfur compounds completed by various DES.....	48
Figure 4.13. DBT molecule .....	49
Figure 4.14. BT molecule. ....	49
Figure 4.15. TS molecule.....	49
Figure 4.16. Different DES and their efficiencies. ....	51
Figure 4.17. Interaction energies for systems 4 and 14. ....	54

# List of tables

Table 2.1 Classification of Deep eutectic solvents.....	5
Table 2.1. List of possible HBDs and salts.....	6
Table 2.3. Freezing points for DES at 101.3 kPa.....	8
Table 2.4. Optimum extraction conditions for DESs.....	17
Table 3.1. Number of molecules used in simulation for different systems.....	33
Table 3.2. Comparison of density and enthalpy of vaporization for the selected components. ...	36
Table 4.1. The energy profile for system 4 at 25 <sup>0</sup> C, 60 <sup>0</sup> C and 100 <sup>0</sup> C.....	46
Table 4.2. The extraction efficiency for different thiophenes. ....	49
Table 4.3. Comparison of systems 11 and 12.....	52
Table 4.4. Interaction energies for systems 13 and 14.....	53



# Chapter 1 - Introduction

Petroleum products play a significant role in daily life; however, it is not a secret that those products carry a lot of polluting compounds which must be removed in an environmentally friendly way. Production of diesel with low content of sulfur became one of the significant challenges for the petroleum industry. Legislation of majority countries in the world requires decreasing the allowable limit of sulfur concentration in fuels and middle distillates to as low as 10 ppm and beyond [1]. The conventional method of sulfur content reduction is hydrodesulfurization (HDS) process. However, the process has its own drawbacks, such as use of elevated temperatures 300-400 °C, high pressure varying from 30 atm to 130 atm, consumption of huge amount of hydrogen, and, complicated aromatic-sulfur compounds such as DBT and TP cannot be totally extracted [2]. These disadvantages of HDS method have pushed towards development of alternative desulfurization techniques, amongst which the most promising development is towards the use of extractive process by suitable solvents.

Recently, several ionic liquids have been suggested to work efficiently to extract sulfur-based compounds from diesel. However, ionic liquids, because of their difficult synthesis, high cost, and questionable toxicity have not been commercialized [3]. On the other hand, more recent focus has been on development

of Deep Eutectic Solvents (DESs) for extractive desulfurization. DESs are considered as greener replacement to ionic liquids. A typical DES consists of at least one hydrogen bond acceptor and one hydrogen bond donor, which results in a mixture with lower melting temperatures than their individual components [4]. Deep Eutectic solvents have a number of beneficial properties such as low vapor pressure, good solubility and also, they can be easily recovered by anti-solvents like water, methanol, or ethanol. Moreover, DESs are considered to be non-flammable, non-toxic, biodegradable and cheap in terms of synthesis [5]. Considering these favorable properties, several applications of DESs have emerged recently, such as metal processing, CO<sub>2</sub> adsorption, organic synthesis and finally, in oil and gas industries, including the use of DESs to extract thiophenic compounds from diesel.

DESs consist of non-symmetric ions which are large because of the complicated structure and they have low lattice energy, thus low melting points. The reason of melting point decrease is that the charge is delocalized via hydrogen bonding between the hydrogen donor and negative ions. Considering a binary mixture of components A and B it can be said that the melting point is decreasing in the direct proportion with increase of interaction between those components [6].

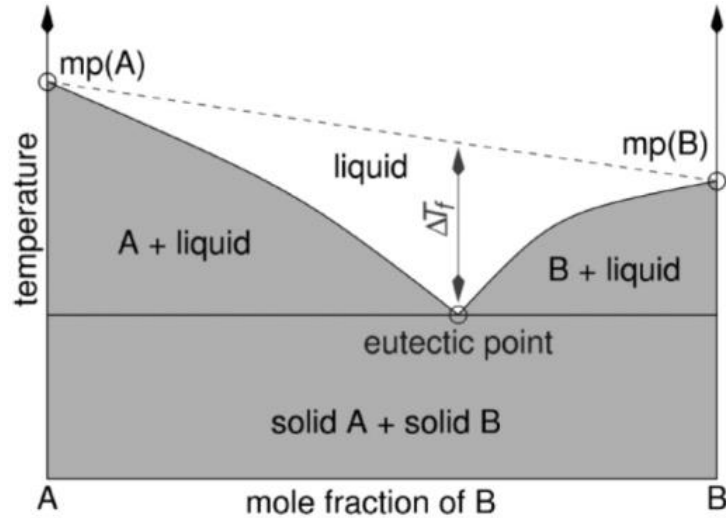


Figure 1.1. Formation of eutectic point in a phase diagram [6].

## 1.1 Objective

In this work, molecular dynamics simulation was used to focus on the formation mechanisms of a DES, which has been proposed as an efficient solvent to extract the refractory compounds from model oils. Moreover, the intermolecular interaction between the DESs, diesel, and thiophenic compounds was explored to understand the extraction process, as existing research works cover only experiments on desulfurization process. Combination of tetrabutylammonium chloride (TBAC), polyethylene glycol (PEG-200), and  $\text{FeCl}_3$  at a ratio of 4:1:0.05 was applied as DES, while octane was used to model diesel. The following mixture had been reported to extract thiophenic compounds with an efficiency ranging from 81% to ~100%, even at very low concentrations and room temperatures, as we discuss later [7].

Dibenzothiophene (DBT), benzothiophene (BT) and thiophene (TS) were used in molecular dynamics simulation representing the sulfur compounds.

In the following thesis, the properties of DESs, its application in industry, and the simulation methodology of the desulfurization process with use of GROMACS tool are reported in chapter 1 and 2. Then the focus will be put on the formation dynamics of DES, its interactions with the octane and DBT molecules in chapter 3. Also, this work will be investigating how different parameters affect the extraction process, such as operating temperature of the system, initial concentration of the DBT, the choice of sulfuric compound and finally, the composition of DES. The concluding remarks and possibilities for the future work will be analyzed in the end of the thesis.

# Chapter 2 – DESs and their applications in desulfurization

## 2.1 Deep eutectic solvents

For the last decade, a significant research was done to investigate the novel solvents called deep eutectic solvents (DESs) which consist of two or more components, that interacting with each other through hydrogen bonds, result in a lower melting point than its individual components [8]. The first work on DES came in 2004, wherein Abbott et al. report a mixture of choline chloride and urea at 1:2 molar ratio, and the resultant mixture showed depression in melting point of more than 200 °C [9]. Depending on the type of components used to form the solvents, DES can be categorized into four groups:

Table 2.1. Classification of Deep eutectic solvents [8].

type	general formula	terms
I	$\text{Cat}^+\text{X}^-\text{zMCl}_x$	$\text{M} = \text{Zn, Sn, Fe, Al, Ga, In}$
II	$\text{Cat}^+\text{X}^-\text{zMCl}_x \cdot y\text{H}_2\text{O}$	$\text{M} = \text{Cr, Co, Cu, Ni, Fe}$
III	$\text{Cat}^+\text{X}^-\text{zRZ}$	$\text{Z} = \text{CONH}_2, \text{COOH, OH}$
IV	$\text{MCl}_x + \text{RZ} = \text{MCl}_{x-1}^+ \cdot \text{RZ} + \text{MCl}_{x+1}^-$	$\text{M} = \text{Al, Zn}$ and $\text{Z} = \text{CONH}_2, \text{OH}$

The general formula for DES is  $\text{Cat}^+\text{X}^-\text{zY}$ , where  $\text{Cat}^+$  is basically ammonium, phosphonium or sulfonium cation, while  $\text{X}^-$  is a Lewis base and it is bonded with z molecules of Y which is a Lewis or Bronsted acid. The type I of DES is a mixture

between quaternary ammonium salt and metal chloride. The type II consists of quaternary ammonium salt and metal chloride hydrate which have relatively low cost. Type III is made of quaternary ammonium salt and hydrogen bond donor and it attracts a lot of attention due to the solvation abilities of metal chlorides and oxides. Finally, the last IV type of DES is consisting of metal chloride hydrate and hydrogen bond donor [10].

A list of different hydrogen bond donors and salts created by García et al. (2015) is presented in the table below:

Table 2.2. List of possible HBDs and salts [11].

<b>HBD</b>	<b>Salts</b>
urea	choline chloride
ethylene glycol	choline nitrate
glycerol	ethylammonium chloride
PEGs	tetrabutylammonium chloride
glucose	tetrabutylammonium bromide
xylitol	benzyltriphenylphosphonium chloride
malonic acid	methyltriphenylphosphonium bromide
arginine	1-butyl-3-methylimidazolium chloride
lactic acid	
phenol	
monoethanolamine	
FeCl <sub>3</sub>	
ZnCl <sub>2</sub>	

## 2.2. Formation of DES

Some deep eutectic solvents are limited in the process application as they have high viscosity and consequently, low conductivity in comparison with aqueous electrolytes [12]. In order to understand the formation of DES and to develop new DESs with low viscosities, Abbott et al. proposed a *Hole theory*. The theory analyzes the movement of ions inside the DES and calculates different physical properties such as density, surface tension, viscosity and conductivity. Hole theory claims that during melting, vacant places are formed because of fluctuations, which are thermally generated in local density and have constant flux. So, for an ion which has a smaller size it is much easier to move into a hole and thus, in this case liquid will have low viscosity [9].

To predict the viscosity of DES it is supposed that holes are still not formed, however, they exist and move in the opposite side to solvent ions. At any time, a DES will have a hole size distribution and if there is a hole with suitable dimension an ion will be moving to it. This means that only some part of ions will be able to move and consequently, the viscosity of DES can be decreased insignificantly. However, it was found that with higher temperature the hole sizes are bigger and it leads to lower viscosities. Basically, knowing the probability of hole formation in the liquid it is easy to generate DES with low viscosities [10].

Beyond the hole theory and its application to design novel DESs, it is also worth to mention about the existence of hydrogen bonds interactions between hydrogen bond donor and hydrogen bond acceptor in DES [13]. Molar ratio between HBD and HBA plays significant role in determination of eutectic point. From the table below, it can be clearly seen that the difference in melting points depends on the molar ratio:

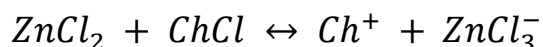
Table 2.3. Freezing points for DES at 101.3 kPa [13].

	mol % BTEAC	freezing point (K)
DES A	20	292
	30	275
	40	279
	50	289
	60	293
	70	314
DES B	30	308
	40	301
	50	299
	60	300
	70	330
DES C	30	301
	40	284
	50	278
	60	306
	70	335

Where, DES A is a mixture of benzyl triethylammonium chloride (BTEAC) and p-toluene sulfonic acid (PTSA), DES B is TEAC with citric acid (CA), DES C is BTEAC and oxalic acid (OX). As visible, the ratio of BTEAC (hydrogen bond donor) affects the melting point of the formed DESs.



However, not all deep eutectic solvents have hydrogen bonds and a freezing point is determined by exchange of ions between compounds and complex structure generation. For instance, Abbot et al. in their research work studied the formation of choline chloride: zinc chloride DES (ChCl:ZnCl<sub>2</sub>), where ions pass the equilibrium reaction [14]:



Chloride anion is a strong base and it shifts the reaction to the right resulting in formation of  $\text{ZnCl}_3^-$ . Furthermore, Mjalli and Shah, continued their research by suggesting that formation of this new ion complex causes the decrease of melting point and formation of DES by affecting the intermolecular interactions [15].

### **2.3 Application**

Due to their unique properties, DESs have found wide range of application in several industries, such as metal processing, gas adsorption, organic synthesis, and in the oil & gas industry. One of the significant advantages of deep eutectic solvents is that they are liquid at the ambient temperature, have low volatility, non-toxic, biodegradable, high conductivity, and have good solubility of metal salts, and are thus reasonable choice for solvents in several processes [16]. Some of these applications are briefly described below.

### ***2.3.1 Metal processing***

One of the current application of DES in metal processing is electroplating, a process during which one of the electrode is covered by metal coating formed by dissolved metal cations reduced due to electric current. Nowadays, different metals such as Zn, Ni, Cr, Co, Cu, Ag, and Au are used in electroplating processes. There are several vital criteria for electroplating process such as low cost, high solubility of metal compounds, conductivity, non-flammability and electrochemical stability. As it was mentioned before, DESs have high solubility for metal salts, oxides and hydroxides, which means that application of DESs can avoid the passivation issues which occur because of formation of non-soluble compounds at the electrodes surface [6].

Moreover, the use of DES does not require the consumption of hazardous complexing agents, for example, cyanide which is toxic and has high disposal cost. Additionally to that, water, which is currently used, is not totally a green solvent, in spite the fact that it is non-toxic, as it requires treatment measures before being disposed to the water courses [10].

Another application is metal electropolishing, an electrochemical process which controls dissolution of a metal workpiece resulting in decrease of surface roughness and increase of optical reflectivity. The current methods to polish the metallic surfaces are using phosphoric and sulfuric acids with different additives such as

CrO<sub>3</sub>. Despite that the majority of those methods are successful there are some limitations such as high toxicity of solutions used and high level of gas evolution which leads to poor current effectiveness [6].

There are several advantages of using deep eutectic solvents over conventional aqueous acid based solutions in the electropolishing process. One of them is minor gas evolution at the interface between anode and solution leading the current efficiency being high. Moreover, deep eutectic solvents are considered to be soft and non-corrosive in comparison with the common solutions.

Use of DES allows applying the polish not only for stainless steel but also for aluminum, titanium, nickel/cobalt and super alloys. One of examples of DESs that has been commercially applied for electroplating is choline chloride with ethylene glycol, which has a freezing point of 10 °C [10].

### ***2.3.2 Organic synthesis application***

In organic synthesis, completing a process in environmentally friendly way is crucial; therefore the choice of solvents plays a vital role. Deep eutectic solvents can find huge application in synthesis process because they are “green”. Shankarling et al., for example, applied chlorine chloride/urea mixture as DESs for bromination, Perkin reaction, and reduction of epoxides [17]. The mechanism of those reactions can be seen in Figure 2.1. Commonly, the synthesis of those products requires use

of strong acids, toxic solvents, and elevated temperatures and authors showed that DESs can be a good alternative to avoid those issues. Moreover, Shankarling with his research group has also used DESs for N-alkylation of aromatic amines for selectivity purposes (Figure 2.2.)

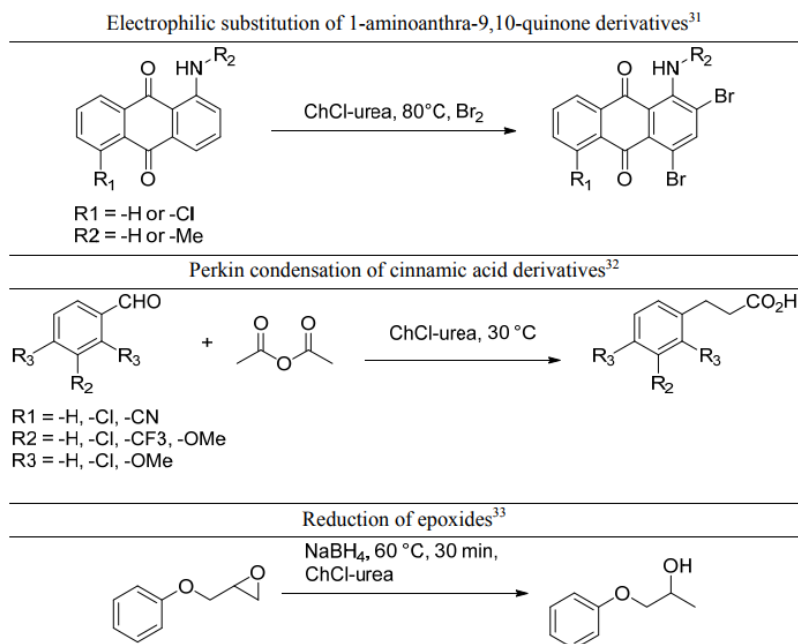


Figure 2.1. Use of ChCl/urea in organic reaction [10].

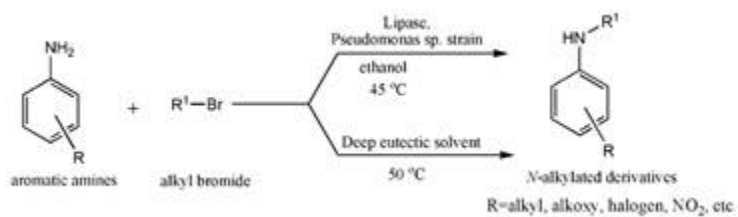


Figure 2.2. Selective N-alkylation of aromatic amines [18].

Another example of applying DESs is choline chloride/zinc chloride in 1:2 molar ratio for Fischer indole annulation performed by Morales et al. in 2004. The

conventional method is carried in hot polyphosphoric acid which is followed by addition of water in order to complete filtration of the product. The disposal of acid residues may bring a negative impact to the environment. However, use of DES can help to avoid this issue and moreover, can give high yield of desirable products [19].

### ***2.3.3 Gas adsorption***

The consumption of fossil fuels grows every year with increase of energy demand and with this accumulation of carbon dioxide increases as well. One of the current methods which is used for carbon capture and store (CCS) is adsorption by solvents like ethanolamine, or by activated carbon, zeolite, or the novel polymeric adsorbents [20].

Considering that some adsorbents cannot be easily synthesized due their toxicity and expensive cost of the process, DESs were suggested as an alternative. Zulkurnai et al. in their work used activated carbon prepared from a sea mango mixed with choline chloride/glycerol in 1:2 molar ratio. The adsorbent showed a high CO<sub>2</sub> adsorption capacity [21].

Another work was accomplished by Zhu et al., wherein the synthesis of cyclic carbonates from carbon dioxide was carried using ChCl/urea (a DES) as a catalyst supported on molecular sieves. This DES could also convert epoxides into cyclic

carbonates (Figure 2.3). After the process was completed the catalyst could be easily extracted and reused as it was insoluble in the products [22].

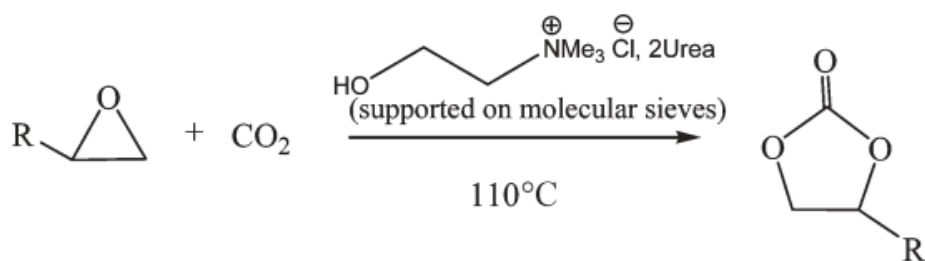


Figure 2.3. Reaction between epoxide with CO<sub>2</sub> in the DES [22].

Zubeir et al. used tetramethylammonium chloride with lactic acid in molar ratio 1:2 as environmentally friendly and biodegradable solvent for CO<sub>2</sub> capture. DES showed excellent performance based on the thermophysical properties and moreover, had a high adsorption capacity [23].

### 2.3.4 Oil and gas industry

Level of aromatic content in fuels is always under constant control because it may harm the environment or cause plugging of equipment. In addition, aromatics form azeotropes with aliphatic hydrocarbons and thus make extraction process very challenging. Nowadays, different extractants such as sulfone and ethylene glycol are used in this process, however, those components are toxic, volatile and flammable. Therefore, use of “green” solvents may be a good alternative to avoid those issues [24]. For example, Rodriguez et al. observed phosphonium-based DES, while another research group lead by Gonzales used choline chloride based DESs as a

solvent in the extraction process and the extraction efficiency in both cases was high [25], [26].

Additionally, DES can be used to extract glycerol from biodiesel which is clean burning fuel made from vegetable oils or animal fats. Biofuel consists of long chain alkyl esters and it is produced through catalyzed transesterification. The by-product of this process is glycerol and it increases the viscosity which may cause damages in the injection parts of diesel engines. Currently, water is used to wash glycerol away from the fuel, however, there is a product loss and moreover, very often this water is disposed without treatment procedures. Abbott et al. tried to implement ammonium salt as a hydrogen bond acceptor and glycerol as a hydrogen bond donor in 1:2 molar ratio and glycerol extraction from the fuel achieved 99 % [27].

Finally, DESs have been also used in sulfuric component extraction such as benzothiophene, dibenzothiophene and thiophene from the conventional fuel. The Chapter I covered the existing desulfurization methods and this chapter, now onwards, will focus more on the sulfur extraction processes using deep eutectic solvents.

Several articles came since 2013 on the applications of deep eutectic solvents in desulfurisation of oil. Most of these articles focus on the use extractive process for

deep desulfurization of fuels and the efficiency of the processes could reach 99% depending on the chosen solvents.

Li et al., for example, were suggesting to apply different combinations of tetrabutylammonium chloride (TBAC) or choline chloride (ChCl) as HBA with malonic acid (MA), tetraethylene glycerol (TEG), ethylene glycol (EG), polyethylene glycol (PEG), glycerol (Gl) or propionate (Pr) as HBD in different molar ratio (1:1 or 1:2). In this process n-octane was chosen as model oil and benzothiophene (BT) with 1600 ppm concentration as a sulfur compound. Desulfurization reaction was lead at 25 °C for 30 minutes with 1:1 mass ratio of DES to model oil. As a result the most effective DES was a combination of TBAC and PEG which could reach 82.83% sulfur removal for one cycle and 99.48% after fifth cycle [28].

The research group lead by Tang, synthesized DES with addition of aluminum chloride ( $\text{AlCl}_3$ ), chlorinated paraffins-52 ( $\text{C}_{12}\text{H}_{19}\text{Cl}_7$ ) and aromatic compounds such as benzene ( $\text{C}_6\text{H}_6$ ), toluene ( $\text{C}_7\text{H}_8$ ), p-xylene ( $\text{C}_8\text{H}_{10}$ ), o-xylene ( $\text{C}_8\text{H}_{10}$ ), ethylbenzene ( $\text{C}_8\text{H}_{10}$ ) and chlorobenzene ( $\text{C}_6\text{H}_5\text{Cl}$ ). DES consisting of paraffins-52, aluminum chloride, and toluene (DES-T) in 1:6:18 molar ratio was chosen for the further analysis. N-heptane was taken as a model oil compound with 3-methylthiophene (3-MT), benzothiophene (BT) and dibenzothiophene (DBT) sulfur content with 500 ppm concentration. The reason DES-T was chosen as a working



material is that it showed the best performance in sulfur extraction: 99.81% for 3-MT, 99.65% for BT and 89.64% for DBT, while the other DESs could reach only 71.64%, 26.63% and 11.93%, respectively [29].

Furthermore, Gano et al. used ferric chloride and tetra-n-butylphosphonium bromide (TBPB) to synthesize DES. The DES was prepared with two different molar ratio, the first DES used  $\text{FeCl}_3$ :TBPB in molar ratio 1:2 (DES 1) and for the second DES 1:1.5 (DES 2). The authors used numerical method to define the most efficient combination of temperature, time and mass fraction and optimized results can be seen in the table below:

Table 1.4. Optimum extract conditions for DESs [30].

Extraction time (mins)	163	180
Extraction temperature (0C)	30.0	50.0
Solvent mass fraction	0.540	0.530
Desirability	0.538	0.553
DBT extraction (predicted, %)	70.4	64.1
DBT verification (measured, %)	71.7	65.0
Relative difference (%)	1.30	0.900
Thiophene extraction (measured, %)	49.8	55.0
Thiophene verification (measured, %)	48.5	53.2
Relative difference (%)	1.30	1.80

In their work, to prepare DESs chemicals were mixed in corresponding molar ratios and were places in an incubator shaker at 80 °C under 1 bar pressure and 270 rpm mixing speed. To form model fuel, n-decane, cyclohexane, iso-octane and toluene were 29.79%, 29.79%, 29.79%, 10.63%, mole percent respectively, and a sulfur

molecule thiophene and DBT with 500 ppm concentration of each was mixed. By applying DES 1 and DES 2, the sulfur extraction after the first cycle was observed to be 64% and 44% respectively, while for the real fuel 32% of the sulfur was extracted.

The same DESs were further applied by Shah and Mjalli, where they used GROMACS simulation tool to view the interaction forces between DESs and sulfur compounds in fuel. The simulation was completed using the same molar ratios, atmospheric pressure, and temperature was chosen to be 343 K, and their results showed that TBP ion had a very strong interaction with the sulfur compounds [15].

The research group headed by Jiang et al. also synthesized different DESs to extract sulfur compounds from fuel. In particular, a mixture of 1-methylimidazole (MIM) or diethanolamine (DEA) (as HBAs) with propanoic acid (PA) or (NA) (as HBDs) was synthesized and as a result MIM/PA performed the best results in sulfur removal efficiency. The authors used equimolar quantity of HBD and HBA, in an inert atmosphere (Ar), at 50 °C to preparing the DESs. To prepare the model oil, n-octane was chosen as a fuel and the following sulfur compounds were mixed: DBT (500 ppm), BT (250 ppm), 4,6-DMDBT (250 ppm) and 1-dodecanethiol (RSH) with 250 ppm concentration. In the extraction process 1.75 g of DESs and 5 ml of model oil was taken. A temperature of 30 °C was chosen for mixing, except for MIM/NA, where in the temperature was 60 °C because of the melting point of the DES.

Extraction time was 10 minutes for MIM/NA and MIM/PA, while for DEA/PA system was 20 minutes due to its high viscosity. Taking a sulfur partition coefficient ( $K_N$ ) as a reference point for sulfur removal efficiency MIM/PA showed the best performance ( $2.31 \text{ mg}_s\text{g}_{IL}^{-1}/\text{mg}_s\text{g}_{oil}^{-1}$ ), while DEA/PA had  $0.43 \text{ mg}_s\text{g}_{IL}^{-1}/\text{mg}_s\text{g}_{oil}^{-1}$  and MIM/NA achieved only  $0.21 \text{ mg}_s\text{g}_{IL}^{-1}/\text{mg}_s\text{g}_{oil}^{-1}$  [30]:

$$-K_N = \text{mg}(\text{sulfur})\text{g} \frac{\text{mg}(\text{sulfur})\text{g}^{-1}(\text{IL})}{\text{mg}(\text{sulfur})\text{g}^{-1}(\text{oil})} \quad (2.1)$$

Li et al., more recently, in their report used metallic based deep eutectic solvents to extract sulfur compounds. The research group tried different HBA and showed that tetrabutylammonium chloride (TBAC) is the most efficient (the other compounds were,  $\text{TBAC} > \text{TEAC} > \text{ChCl}$ ) while for HBD polyethylene glycol was chosen as the best among propionic acid (Pr), glycol (GL), malonic acid (MA), benzoic acid (BA) and formic acid (FA) in respective order of decreasing efficiency. In addition, the authors also used metallic salt as a third component in the DESs. Regarding the metallic ions ferric chloride showed the highest performance in comparison with zinc, copper, cobalt and nickel chlorides resulting 89.53% removal efficiency per one cycle. So, the combination of TBAC:PEG:FeCl<sub>3</sub> was taken for the further analysis with 4:1:0.05 molar ratio respectively. N-octane with ~2000 ppm of dibenzothiophene was used as the model oil. Figure 2.4 shows that TBAC:PEG:FeCl<sub>3</sub> has the highest extraction efficiency, while from Figure 2.5 it can

be seen that the efficient molar ratio between the compounds was found to be 4:1:0.05 respectively [31].

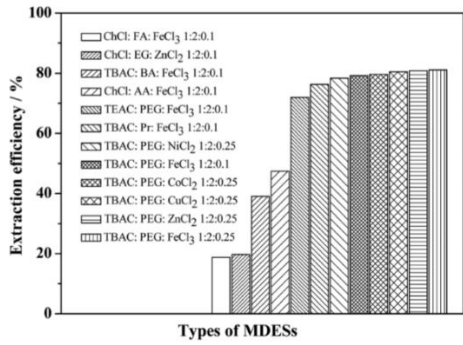


Figure 2.4. MDESs and their efficiencies.

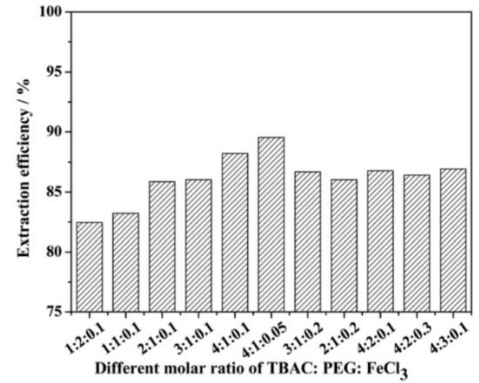


Figure 2.5. Molar ratio for DES.

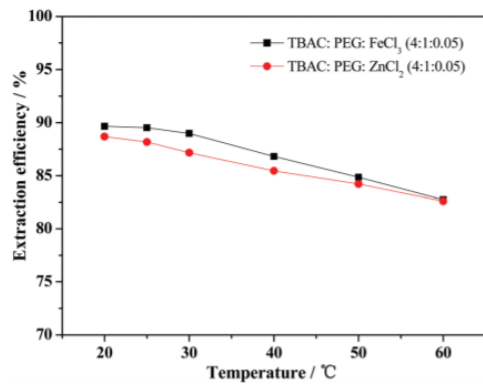


Figure 2.6. Effect of temperature on the efficiency.

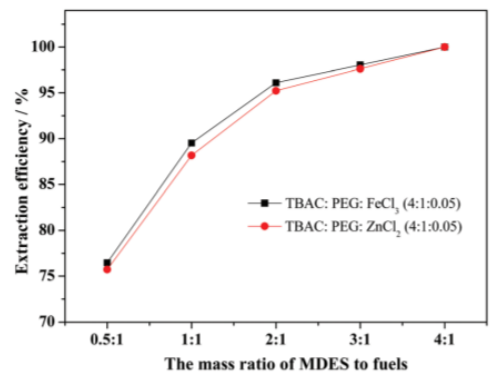


Figure 2.7. Effect of mass ratio on the efficiency.

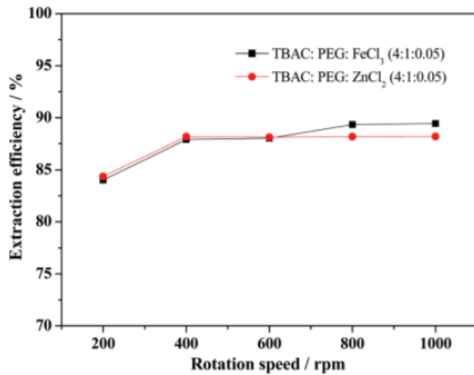


Figure 2.8. Effect of mixing speed on the efficiency

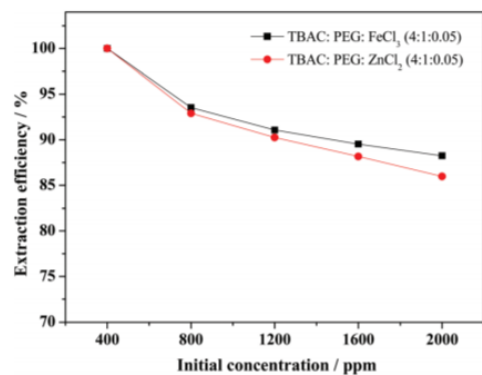


Figure 2.9. Effect of sulfur concentration on the efficiency.

Different parameters such as temperature, mass ratio between oil and DESs, mixing velocity and initial concentration of DBT were investigated. So, as it can be seen from the figures above increase of temperature and initial sulfur concentration leads to desulfurization efficiency decrease. However, with increase of mass ratio between model oil and DES the removal sulfur activity also rises. Finally, variation of mixing speed showed that there is a sharp rise of efficiency at 400 rpm, while after increase of speed does not lead to any changes.

Further, Li et al. synthesized carboxylic acid-based DESs, for example, TBAB/HCOOH to extract sulfur compounds such as thiophene (TS), dibenzothiophene (DBT), and benzothiophene (BT) from model oil. To prepare DESs the raw materials were mixed and heated at 80–90 °C temperature for 2-3 hours. Those solvents were added to model oil (n-octane) which contained dissolved sulfur molecules with 500 ppm concentration. The extraction process was lead under 30 °C temperature for 40 minutes. So, from different carboxylic acids which served as HBAs, formic acid based DES showed good sulfur removal results with extraction efficiency reaching 81.75%, 80.47%, and 72% in single stage for BT, DBT and TS, respectively and after third cycle increased to 98.32%, 98.24% and 97.6% [32].

Shu et al. in their work used tetrabutylammonium chloride as HBA and different HBA such as ethylene glycol, glycerol and malonic acid to synthesize DESs. N-octane with 1000 ppmw of 2-methylthiophene and benzothiophene was chosen as

model gasoline. Additionally, the group also used real gasoline with 406 ppmw of sulfur content taken from by Sinopec Shanghai Petrochemical Company. To synthesize DES different molar ratio between HBA and HBD were varied between 1:1, 1:2 and 1:3, however, the experiment showed that 1:2 is the best option for the extraction process. By further analysis it was found that TBAC/ethylene glycol is more efficient than TBAC/glycerol and TBAC/malonic acid and it leads to conclusion that alcohol based hydrogen bond donor is more favor than acid-based HBD. The research group investigated the extraction efficiency of those DESs for desulfurization process of real gasoline and the results showed 38.7%, 31.5% and 26.3% for TBAC/ethylene glycol, TBAC/glycerol and TBAC/malonic acid, respectively. After 5 cycles the results were 85.7%, 76.9% and 71.4%, while extraction performance for model fuel is 99.5%, 99.3% and 99.2%, respectively [33].

Jiang et al. suggested to use extractive method to remove sulfur compound by applying choline chloride-based DESs. BT, 3-MBT, DBT, 4-MDBT, and 4,6-DMDBT were chosen as sulfur compounds with 500 ppm concentration in n-octane which was served as a model oil. DESs were represented as the following chemical compounds:  $[C_4DMEA]Cl/FeCl_3$ ,  $[C_8DMEA]Cl/FeCl_3$ ,  $[C_{12}DMEA]Cl/FeCl_3$ ,  $[BzDMEA]Cl/FeCl_3$  and  $[BzMDEA]Cl/FeCl_3$ . The DESs were mixed with oil and were magnetically stirred for 10 minutes in water bath. As the results showed the

most efficient DES was [C<sub>12</sub>DMEA] Cl/FeCl<sub>3</sub> with 52.9% extraction in one step and up to 99.3% after five steps (see figure 2.10 below).

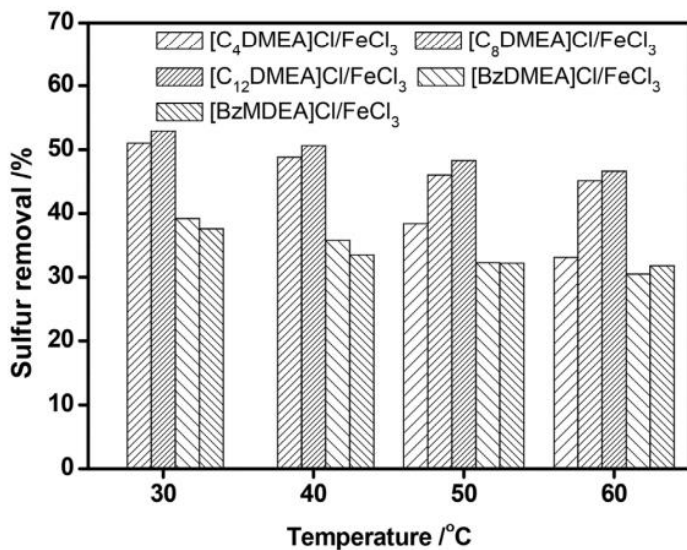


Figure 2.10. DBT removal by different DESs (1g) for 10 minutes from model oil (5 mL) [34].

Using different sulfur components in model oil showed different extraction abilities (as shown in Figure 2.11). As observed from the figure, 4,6-DMDBT can be extracted till 35.7% at the first step, whereas for DBT the extraction was about 53%.

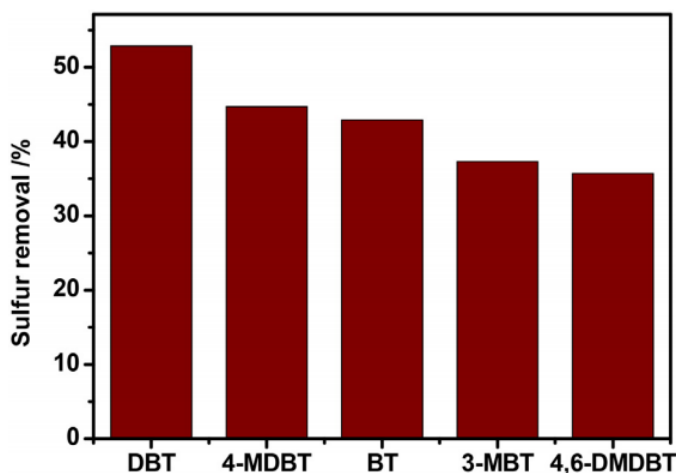


Figure 2.11. Different sulfur compounds removal by [C<sub>12</sub>DMEA]Cl/FeCl<sub>3</sub> at 30 °C for 10 min [34].

Further, Ani et al. suggested use of tetra-butylammonium bromide (TBAB) and polyethylene glycol 200 as a deep eutectic solvent in 1:2 molar ratio, respectively and conducted the experiment in continuous liquid–liquid microchannels having 1.22 mm ID of the glass channel at room conditions. The fuel was prepared with the following composition: 29% of iso-octane ( $(\text{CH}_3)_3$ ), 29% of n-decane ( $\text{CCH}_2\text{CH}(\text{CH}_3)_2$ ), 29% of cyclohexane ( $\text{C}_6\text{H}_{12}$ ) and 13% of toluene ( $\text{C}_7\text{H}_8$ ) and DBT with 200 ppm concentration was chosen as a sulfur compound. The extraction efficiency was achieved to be almost 80% after one cycle [35].

Recently, tetrabutylammonium bromide (TBAB) as a hydrogen bond acceptor and polyethylene glycol with different molecular weight, namely, PEG-600 and PEG-200 as a hydrogen bond donor was also applied in the desulfurization process [36]. The model oil consisted of cyclohexane (29 wt%), iso-octane (29 wt%), n-decane (29 wt%) and toluene (13 wt%). As sulfur compound dibenzothiophene (DBT) and thiophene (TP) were chosen in total concentration 500 ppm (w/w). The extraction results showed that by using volume ratio of 1:1 between DES and fuel the sulfur compounds can be extracted by 82.40% and 62.16% for DBT and TP respectively after the first stage.

In summary, we observe from all of the above-mentioned studies that DESs have great potential in desulfurization and that different parameters such as operating temperature, speed of mixing, extraction time, initial concentration of sulfur in fuel



had an effect on sulfur extraction. Among the different operation parameters, we observe that high temperature is not beneficial for the processes. The mixing time was, although different for different system was, in general, low. While high mixing velocity could assist and make the process faster, it was avoided so as to control the bubble formation during the extraction process. About initial sulfur concentration, there are conflicting opinions. Certain reports indicate that with an increase of initial sulfur content the extraction efficiency decreases, however, others observe no change in the extraction efficiency with variation in the sulfur concentration. Lastly, there were discussions on regeneration of DES by applying different anti-solvents, which has not been discussed herein, to maintain brevity.

# Chapter 3 - Simulation methodology

## 3.1 Molecular dynamics simulation

Molecular dynamics simulation is a computational method which allows observing the molecules' behavior inside the system by simulating their movements. Basically, the molecular dynamics follows the Newtonian laws of motion subjected to potential energy ( $U(r)$ ), originating because of the intermolecular interaction [37].

$$f_i = -\nabla_{r_i} U(r) = m_i d^2(r_i)/dt^2 \quad (3.1)$$

where,  $m_i$  the particle mass and  $a_i$  is its acceleration. The total energy of the system containing  $N$  molecules is comprised of kinetic ( $K$ ) and potential energies ( $U(r)$ ):

$$H = K + U(r) \quad (3.2)$$

Where  $K$  is:

$$K = \sum_{i=1}^N m_i v_i^2 / 2 \quad (3.3)$$

And  $U(r)$  is summation of different energies:

$$U(r) = U_{\text{bond}} + U_{\text{angle}} + U_{\text{UB}} + U_{\text{dihedral}} + U_{\text{improper}} + U_{\text{LJ}} + U_{\text{C}} \quad (3.4)$$

Where  $U_{\text{bond}}$  is the energy which stored in covalent bonds in the system. Each bond is characterized by a harmonic spring with specific force constant ( $K_b$ ), actual length bond  $b$  and the equilibrium length bond  $b_0$ :

$$U_{bonds} = \sum_{bonds} K_b (b - b_0)^2 \quad (3.5)$$

Another term which contributes to the total potential energy is  $U_{angle}$  which is the valence angle energy generated when the angle between two covalent bonds ( $\theta$ ) moves from its initial position  $\theta_0$  with  $K_\theta$  angle force constant:

$$U_{angle} = \sum_{angles} K_\theta (\theta - \theta_0)^2 \quad (3.6)$$

The following parameter  $U_{UB}$  corresponds to Urey-Bradley component which is a cross-term accounting for atoms experiencing nonbonded interactions, where  $s$  is the distance between separated atoms,  $s_0$  is the equilibrium distance and  $K_S$  is the respective force constant:

$$U_{UB} = \sum_{UBs} K_S (s - s_0)^2 \quad (3.7)$$

The next term  $U_{dihedral}$  which is the dihedral interaction energy accounts for the torsional energy surface, where  $K_\varphi$  is the dihedral force constant,  $n$  is the multiplicity factor of the function,  $\varphi$  is the dihedral angle and  $\delta$  is the phase:

$$U_{dihedrals} = K_\varphi (1 + \cos(n\varphi - \delta)) \quad (3.8)$$

The fifth term  $U_{improper}$  is the energy of the improper, out of plane torsions, where  $K_\omega$  stands for the force constant and the difference  $\omega - \omega_0$  is the out of plane angle:

$$U_{improper} = \sum_{improvers} K_\omega (\omega - \omega_0)^2 \quad (3.9)$$

The last two terms belong to non-bonded interactions which are Lennard-Jones and Coulomb potentials:

$$U_{LJ} = \sum_{nonbonded\ pairs} \epsilon_{ij} \left( \left( \frac{r_{ij}^{min}}{r_{ij}} \right)^{12} - 2 \left( \frac{r_{ij}^{min}}{r_{ij}} \right)^6 \right) \quad (3.10)$$

And,

$$U_C = \sum_{nonbonded\ pairs} \frac{q_i q_j}{4\pi\epsilon_0\epsilon_r r_{ij}} \quad (3.11)$$

Van der Waals interactions are modeled between atoms i and j at distance  $r_{ij}$  through Lennard-Jones (LJ) potential. The minimum LJ energy between atoms with  $\epsilon_{ij}$  value takes place at distance  $r_{ij}^{min}$ .

While the Coulomb potential is responsible for the electrostatic interaction between charges  $q_i$  and  $q_j$ .  $\epsilon_0$  is permeability of vacuum,  $\epsilon_r$  is the relative dielectric constant and usually it is taken as 1 [38].

### 3.2 GROMACS TOOL

Gromacs 5.0 package was used to perform all-atom molecular dynamics simulation for the DES. As it was mentioned before octane and DBT are the main compounds for the model oil while DES is consisted of TBAC,  $FeCl_3$  and PEG, where the last one is chain molecule with chemical formula  $C_{2n}H_{4n+2}O_{n+1}$ . To match the mass and molar ratio n was chosen to be 4 resulting in the molar mass being  $\sim 200$  g/mol.

Optimized coordinates and forcefield parameters for tetrabutylammonium (TBA) ion and PEG-200 were taken from Automated Topology Builder (ATB) database [39]. The interaction parameters for  $\text{Fe}^{+3}$  ion was taken from Lin et al. [40]. All other parameters were taken according to the gromos54a7 forcefield [41]. Simulations were started using a low-density box with  $15 \times 15 \times 15 \text{ nm}^3$  was chosen for the study and the number of molecules were inserted according to specified molar ratio of 4:1:0.05. Specifically, 400 molecules of tetrabutylammonium, 415 molecules of chloride, 100 molecules of polyethylene glycol and finally, 5 molecules of iron were added. In addition, octane (911 molecules) was used as to model diesel and DBT (2 molecules) was used to mimic 2000 ppm of sulfur content in oil. Forcefield parameters from octane and DBT were also taken from the ATB server. Several systems were designed to systematically explore the mechanism(s) of DES formation and the sulfur extraction process.

After creating the initial geometry with the molecules, energy minimization was performed and further NVT-equilibration and NPT-equilibration for 0.2 ns at 298/333 K and 1 bar was completed. The simulations were put to run for 10 ns and only the last 2 ns were used for the equilibrium analysis. During this simulation LINCS constraint algorithm was applied for all the bonds. For Coulomb and Lennard-Jones (LJ) short-range interactions 1.5 nm cut-off was applied. Particle Mesh Ewald summation method was used to calculate long-range interactions with

0.16 nm grid spacing and fourth-order interpolation. The modified Berendsen coupling method was used for maintaining constant temperature at 298/333 K, while pressure was running under Parrinello-Rahman coupling method at 1 bar. Periodic boundary conditions were on during all simulation steps (Figure 3.1). After the simulation was completed Visual Molecular Dynamics (VMD) tool was applied to extract the radial distribution functions and visual models of running systems. All other analysis was performed using Gromacs package.

```

title           = TITLE OF YOUR CHOICE
; define        = -DPOSRES           ; position restrain We are not using it
; Run parameters
integrator      = md                 ; leap-frog integrator
nsteps         = 5000000             ; 2 * 5000000 = 100 ps
dt             = 0.002               ; 2 fs
; Output control
nstxout        = 1000                ; save coordinates every 1.0 ps
nstvout        = 1000                ; save velocities every 1.0 ps
nstenergy      = 1000                ; save energies every 1.0 ps
nstlog         = 1000                ; update log file every 1.0 ps
nstxout-compressed = 1000           ; xtc
energygrps     =                    _TPH
; Bond parameters
continuation   = yes                 ; Restarting after NVT
constraint_algorithm = lincs         ; holonomic constraints
constraints    = all-bonds           ; all bonds (even heavy atom-H bonds) constrained
lincs_iter     = 1                   ; accuracy of LINCS
lincs_order    = 4                   ; also related to accuracy
; Neighborsearching
cutoff-scheme  = Verlet
ns_type        = grid                ; search neighboring grid cells
nstlist        = 10                  ; 20 fs, largely irrelevant with Verlet scheme
rcoulomb       = 1.0                 ; short-range electrostatic cutoff (in nm)
rvdw           = 1.0                 ; short-range van der Waals cutoff (in nm)
; Electrostatics
coulombtype    = PME                 ; Particle Mesh Ewald for long-range electrostatics
pme_order      = 4                   ; cubic interpolation
fourierspacing = 0.16                ; grid spacing for FFT
; Temperature coupling is on
tcoupl         = V-rescale            ; modified Berendsen thermostat
tc-grps        = System               ; two coupling groups - more accurate
tau_t          = 0.1                 ; time constant, in ps
ref_t          = 298                 ; reference temperature, one for each group, in K
; Pressure coupling is on
pcoupl         = Parrinello-Rahman    ; Pressure coupling on in NPT
;          pcoupl      = Berendsen    ; Pressure coupling on in NPT (use if air)
pcoupltype     = isotropic            ; uniform scaling of box vectors
tau_p          = 2.0                 ; time constant, in ps
ref_p          = 1.0                 ; reference pressure, in bar
compressibility = 4.5e-5              ; isothermal compressibility of water, bar^-1
refcoord_scaling = com
; Periodic boundary conditions
pbc            = xyz                  ; 3-D PBC
; Dispersion correction
DispCorr       = EnerPres            ; account for cut-off vdW scheme
; Velocity generation
gen_vel        = no                  ; Velocity generation is off |

```

Figure 3.1. Simulation worksheet for the Thiophenic compounds.

### 3.3 Systems simulated

In order to get the full picture of desulfurization process, different systems were simulated, wherein, several parameters were varied such as temperature of the system, the choice and the concentrations of the sulfur compounds, and finally, the composition of deep eutectic solvents.

The first system which was simulated was pure TBAC and it was completed to analyze the base case, and identify the interaction energies between TBA and Cl. Simulation of the second system was directed to show the process of DES formation and how melting point was decreased. Later, system 3, which is the model oil consisting of n-octane with ~2000 ppm of DBT, was simulated to understand the strength of interactions between DBT and octane and to prove of necessity for desulfurization process.

Starting from system 4 the desulfurization process was simulated to show that application of TBAC:PEG:FeCl<sub>3</sub> in DBT removal. Moreover, this system was also simulated at 60 °C and 100°C in order to follow the effect of temperature on the process. Later, systems 5, 6, 7 and 8 were simulated to evaluate how increase of sulfur concentration (5000 ppm and 9000 ppm respectively) may affect the interaction between octane and DBT, and the desulfurization process.

Systems 9 and 10 were created to study how extraction activity depends on the different sulfuric derivatives, such as thiophene (TS) and benzothiophene (BT).

Starting from system 11 to 14 the fuel composition was kept the same, while DES content varied in the way that either polyethylene glycol or ferric chloride was removed from the system so that only two components left in the DES. The main aim for running those systems was to study how DES constituents may affect the desulfurization process. So, systems 11 and 12 solvents were represented by TBAC:PEG, while systems 13 and 14 used TBAC:FeCl<sub>3</sub> solvents.

Finally, the last system containing octane with DES was simulated as a negative control in order to determine mixability of fuel with DESs. The results are shown separately in Appendix A.

Using molar ratio between TBAC, PEG and FeCl<sub>3</sub> (4:1:0.05) number of molecules were calculated: 400 for TBAC, 100 for PEG and 5 for FeCl<sub>3</sub>, and knowing the mass ratio between model oil and DESs the number molecules for n-octane was calculated to be 911 with 2 DBT molecules corresponding to ~ 2000 ppm concentration.

The table below provides details of the different systems which were simulated:



Table 3.1: Number of molecules used in simulation for different systems.

<b>System</b>		<b>Number of molecules of</b>						
<b>No.</b>	<b>TBA<sup>+</sup></b>	<b>Cl<sup>-</sup></b>	<b>Fe<sup>+3</sup></b>	<b>PEG</b>	<b>Octane</b>	<b>DBT</b>	<b>TS</b>	<b>BT</b>
<b>1</b>	400	400	-	-	-	-	-	-
<b>2</b>	400	415	5	100	-	-	-	-
<b>3</b>	-	-	-	-	911	2	-	-
<b>4</b>	400	415	5	100	911	2	-	-
<b>5</b>	-	-	-	-	911	5	-	-
<b>6</b>	-	-	-	-	911	9	-	-
<b>7</b>	400	415	5	100	911	5	-	-
<b>8</b>	400	415	5	100	911	9	-	-
<b>9</b>	400	415	5	100	911	-	2	-
<b>10</b>	400	415	5	100	911	-	-	2
<b>11</b>	197	197	-	394	911	2	-	-
<b>12</b>	400	400	-	100	911	2	-	-
<b>13</b>	366	915	183	-	911	2	-	-
<b>14</b>	400	415	5	-	911	2	-	-

The pressure and temperature of all systems were kept constant at 298 K and 1 bar.

Also, system 4 was run at 333 K and 373 K, thus, in total 16 systems were simulated.

### 3.4 Force-field validation

In molecular dynamics simulations the choice of force-field parameters may affect the final results. In order to get an idea how simulated results may be different from the experimental ones, the thiophene compound was selected as a reference for the analysis.

Following the pathway described in section 3.2 a box with 500 molecules of thiophene was simulated:

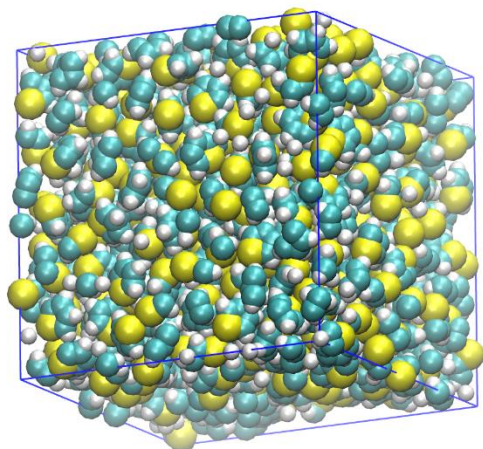


Figure 3.2. Simulated box of 500 thiophene molecules through VMD tool.

By simulating TS molecules at 288 K, 298 K, 307 K and 317 K the temperature dependence density was obtained. From the Figure 3.3 it can be seen that both densities from literature and from the gromacs simulations follow the same trend and there is insignificant difference in their values.

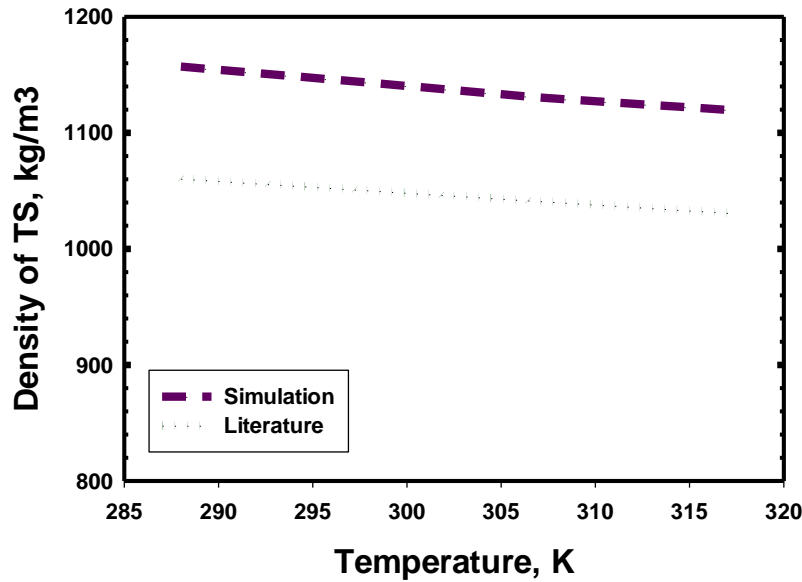


Figure 3.3. Density of TS over temperature.

Moreover, octane, dibenzothiophene, thiophene and polyethylene glycol were simulated separately in order to obtain density ( $\rho$ ) and enthalpy of vaporization ( $\Delta H_{vap}$ ) parameters and to compare them with literature values (Table 3.).

To calculate the enthalpy of vaporization the following formula was used:

$$\Delta H_{vap} = U_v - \frac{U_L}{N} + RT \quad (3.1)$$

Where  $U_v$  is the total potential of the vapor phase,  $U_L$  is the total potential of a liquid phase,  $R$  is a gas constant ( $8.31 \times 10^{-3}$  kJ/mol/K) and  $T$  is the temperature of the system (298 K).

Table 3.2. Comparison of density and enthalpy of vaporization for the selected components.

<b>Component</b>	<b>Enthalpy (kJ/mol)</b>		<b>Density (g/cm<sup>3</sup>)</b>	
	<b>simulation</b>	<b>Literature [42]</b>	<b>simulation</b>	<b>literature</b>
<b>Octane</b>	35.9	34.4	0.744	0.700
<b>DBT</b>	63.2	78.3	1.21	1.30
<b>TS</b>	30.1	31.5	1.14	1.10
<b>PEG</b>	94.8	66.1	1.18	1.10

From the table it can be seen that the values (at 25 °C and 1 bar) taken from the literature and obtained through simulation are quite similar, supporting our choice of the forcefield parameters.

# Chapter 4 - Results and discussion

## 4.1 DES formation

The molecular mechanism of the formation of DES is not clear. In general, the formation of DESs are described in terms of hole theory or in terms of hydrogen bonds. However, in our case, type I DESs, hydrogen bonding is not feasible, and the hole theory does not reveal the molecular picture, Hence, our first aim in this work is to explore the formation mechanism of the DES, i.e., to understand the strong depression in the freezing point observed from the molecular point of view. Therefore in the analysis we start with comparing simulation of pure TBAC (system 1) with the system containing TBAC:PEG: FeCl<sub>3</sub> (system 2).

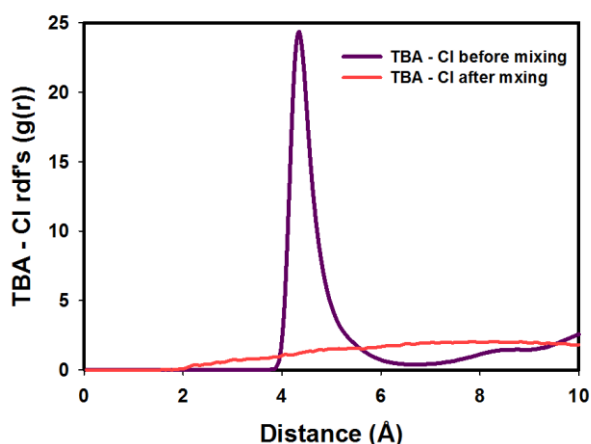


Figure 4.1. Radial distribution functions between TBA ion and Cl ion for system 1 and 2.

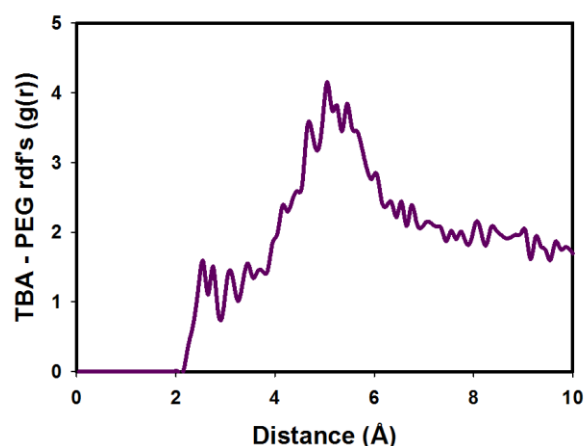


Figure 4.2. Radial distribution function between the TBA ion and PEG for system 2.

The radial distribution functions (rdfs) between different components were determined. The rdfs show the measure of probability for an atom being at the distance  $r$  from the reference atom. Nitrogen atom of the TBA ion, and central oxygen atom of the PEG molecules were chosen as reference to determine the rdfs.

Figure 4.1 shows the rdfs between the central nitrogen atom of the TBA ion with the chloride ion before and after mixing with  $\text{FeCl}_3$  and PEG, i.e., system 1 and system 2. From this figure it can be seen that in system I the first Cl ion appears at distance of 4.35 Å from the central nitrogen atom of the TBA ion and the peak value of  $g(r)$  is 25, however, in system II, the interaction decreased significantly, which can be explained by the fact that TBA ion started to interact with PEG molecule as shown in Figure 4.2. It is also important to highlight that after mixing with PEG and  $\text{FeCl}_3$ , the distance between nitrogen atom and chloride ion decreases with very low peak. The strong decrease in the strength of interactions between the TBA and Cl ions probably causes the strong depression the melting point of the DES.

Moreover, the total interaction energies (sum of LJ and coulombic energies) between TBA and Cl ions of system I were compared with total energy of DES. Figure 4.3 clearly shows that interaction energy of pure TBAC system is much higher than the DES system, which also indicates towards the depression in the melting point observed. We also note that although the difference between the interaction energy

is small, it is significant, as the DES also contain PEG and FeCl<sub>3</sub>, for which pure energies are not shown.

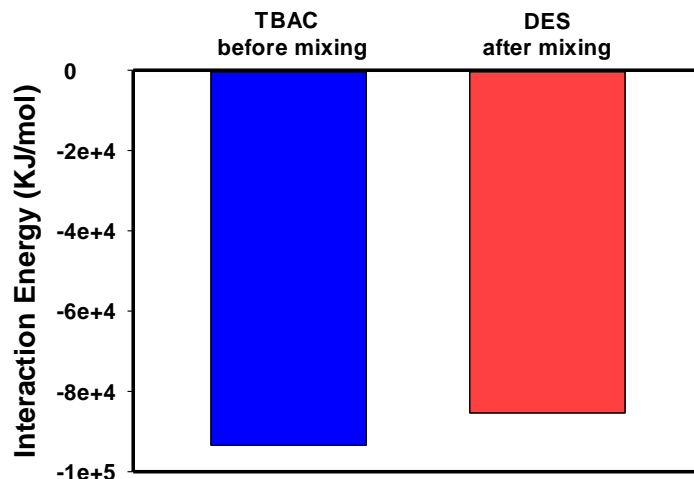


Figure 4.3 Interaction energy profile for TBAC and DES (systems 1 and 2).

## 4.2 Desulfurization process

After understanding the formation of DES, we simulate the model fuel containing ~ 2000 ppm DBT concentration (system 3) to show how strong interaction is between octane and DBT compounds. Running the system with 911 molecules of n-octane and 2 DBT molecules it was found that interaction between them is significantly high (-182 kJ/mol), which means that this interaction must be weakened somehow in order to remove sulfur from the fuel.

A system with DES was mixed with this model oil to analyze the effectiveness of DES in the desulfurization process. Figure 4.4 compares the interaction energy between DBT and n-octane before mixing with DES and interaction energy between

DBT and DES after mixing fuel with deep eutectic solvents. The results show that DES captures the DBT molecules as the DBT-DES system has approximately twice the energy in comparison with the DBT-octane system. In particular, the energy between octane and the sulfur compound was  $\sim 80$  kJ/mol, however, between the DES and sulfur compound was  $\sim 150$  kJ/mol.

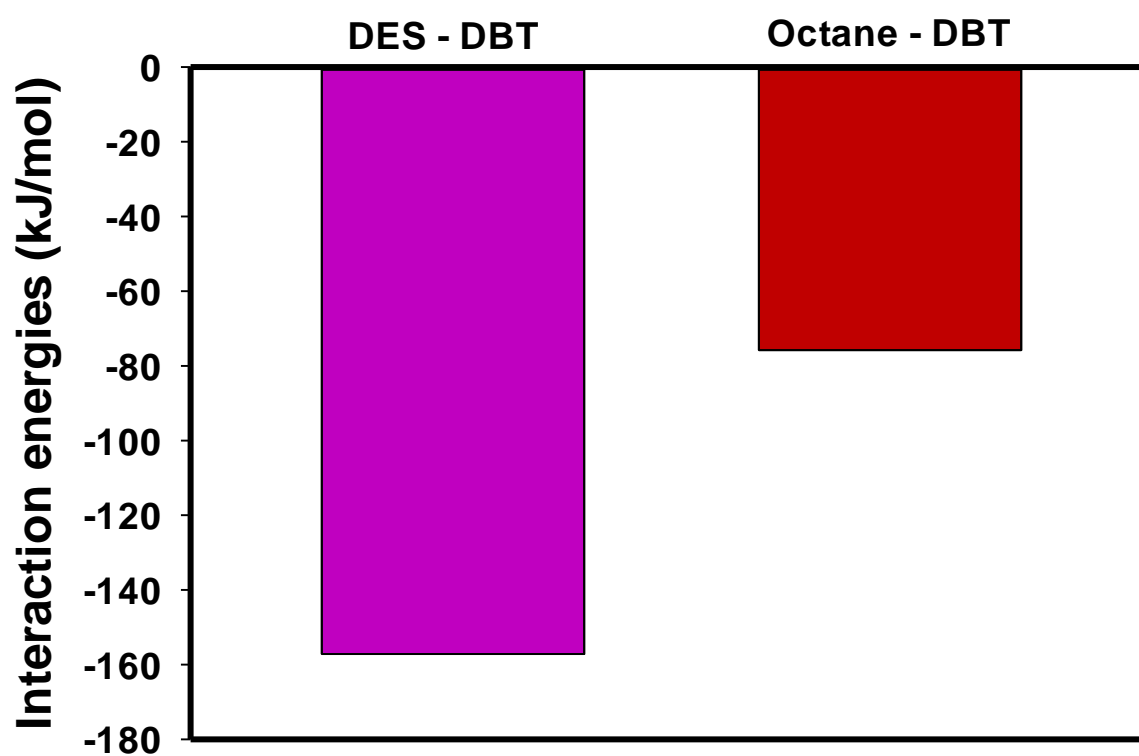


Figure 4.4. Interaction energy profile for DBT-octane and DBT- DES in system 4.

Further analysis of the interaction energies between DBT and DES showed that tetrabutylammonium chloride and polyethylene glycol are the most contributing



agents for the desulfurization process, while ferric atom has almost zero (0.0015 kJ/mol) interaction with the DBT molecule:

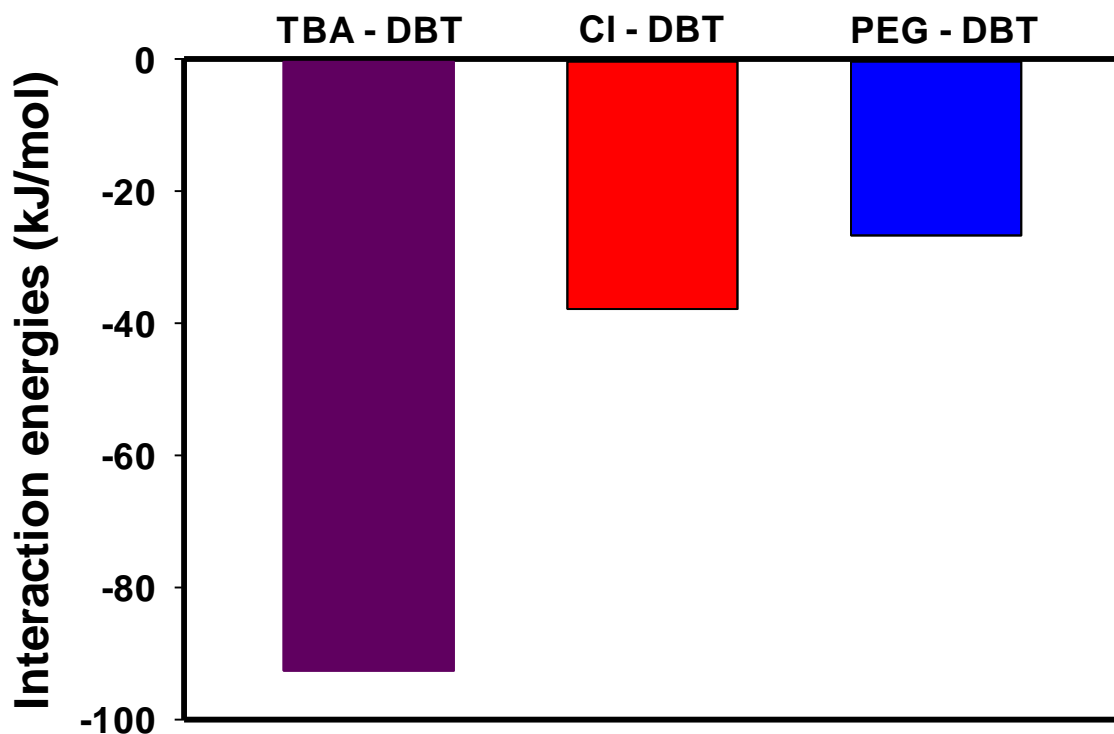


Figure 4.5. Interaction energies for DES compounds with DBT in system 4.

In order to further understand the system, the radial distribution functions were plotted for the dibenzothiophene molecule with octane and deep eutectic solvents after mixing. The central sulfur atom from DBT molecule was taken as a reference, while for octane it was the central carbon atom (C4). The results, as shown in Figure 4.6, indicate that DBT molecules, among all the components present in the system, weakly interacts with octane, but has strong interactions with TBA ion, followed with the PEG molecules.

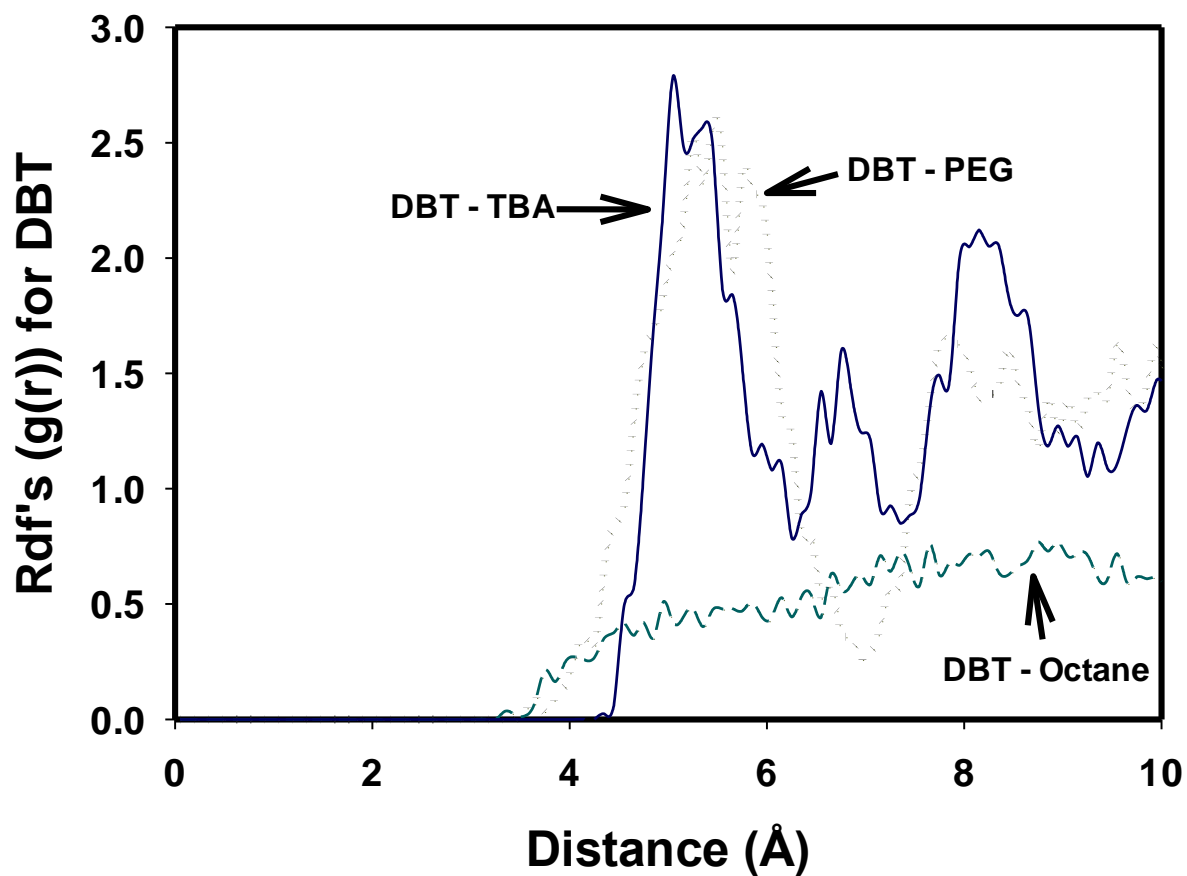


Figure 4.6. Rdfs for DBT with octane, PEG and TBA inside the system 4.

The following figures show the visual representation of desulfurization process, where before mixing DBT molecule was surrounded by octane molecules, while after the process was completed DBT was captured by DES.

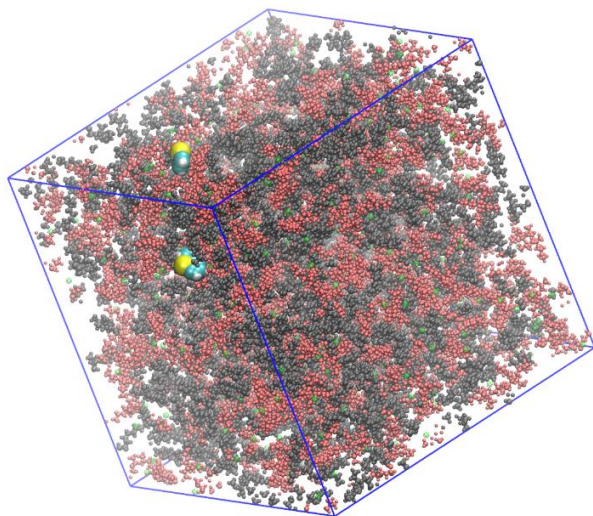


Figure 4.7. DBT molecule surrounded by octane (black).

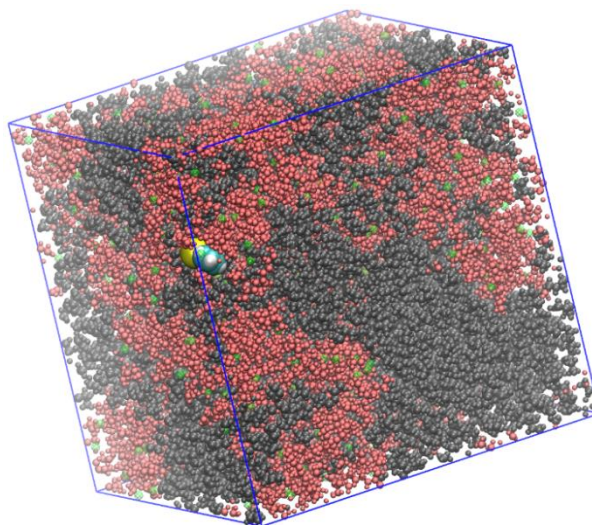


Figure 4.8 DBT molecule captured by DES (red).

### 4.3 Effect of process parameters on extraction process

In this section concentration of dibenzothiophene, effect of temperature on the process was studied. Moreover, DBT will be substituted by thiophene (TS) and benzothiophene (BT) to follow the desulfurization process.

#### 4.3.1 Concentration of the thiophenic compounds

Next, in order to study how initial sulfur concentration affects the extraction process two more systems 5 and 6 were simulated, which contain octane with approximately 5000 ppm and 9000 ppm concentration of DBT (5 and 9 molecules of DBT in 911 molecules of octane). As mentioned above, although the literature uses a concentration of thiophenes of less than 2000 ppm, in simulations we have worked with high values in order to (i) to be able to perform simulations within reasonable

timeframe (ii) to capture the effectiveness of these solvents at high sulfur concentrations. The interaction of DBT with octane was evaluated and as it can be seen from Figure 4.9 rise of sulfur concentration leads to increase of the interacting strength between those molecules from -470.8 kJ/mol to -845.1 kJ/mol. Later, to evaluate if the desulfurization process can be achieved for fuel with higher concentration of DBT, systems 7 and 8 with addition of DES were simulated. The interaction energy between octane and DBT was -158.2 kJ/mol in the system 7 containing 5000 ppm DBT and the energy between DES/DBT was -417.9 kJ/mol. System 8 showed that octane/DBT interaction was -303.9 kJ/mol, whereas DES/DBT was -685.2 kJ/mol, which means that after mixing model oil with DES, the oil/sulfur interaction sufficiently decreases leading to conclusion that DES is able to extract sulfur compounds from the system.

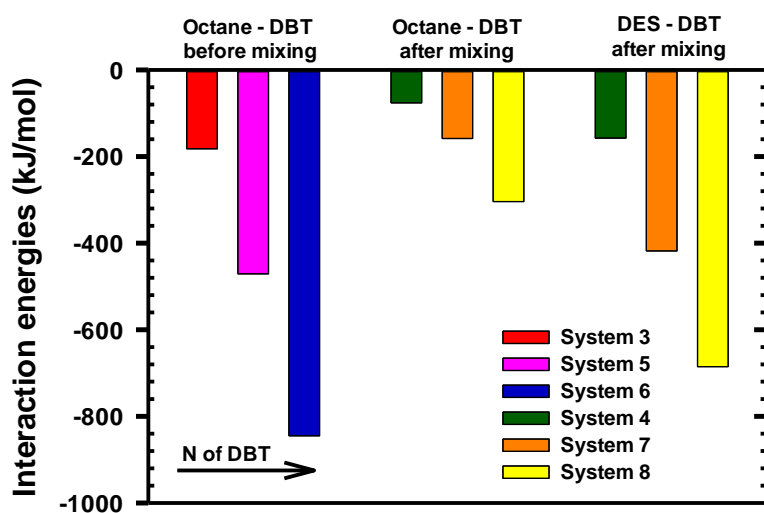


Figure 4.9. The summary of interaction energies for different systems (with increasing DBT concentrations).

Moreover, rdfs analysis for systems 7 and 8 also shows that DBT interacts more with DES rather than with octane. Referring to the interaction energies values for those systems, the most interacting component from DES were TBA ion and PEG, therefore they were chosen for radial distribution analysis which is presented in Figure 4.10 and Figure 4.11. As it can be seen from the pictures the most contributing component to interact with the DBT molecule herein was PEG which had peaks around 4 Å or even higher (for system 8) with highest value of 3.5. TBA could reach peaks value of 2 at 4 Å, while octane showed peak value of 1 at 3 Å for the both systems. Thus, the obtained results may claim that the desulfurization process using TBAC:PEG:FeCl<sub>3</sub> at the molar ratio (4:1:0.05) can be efficiently completed even at high concentrations of sulfur compounds.

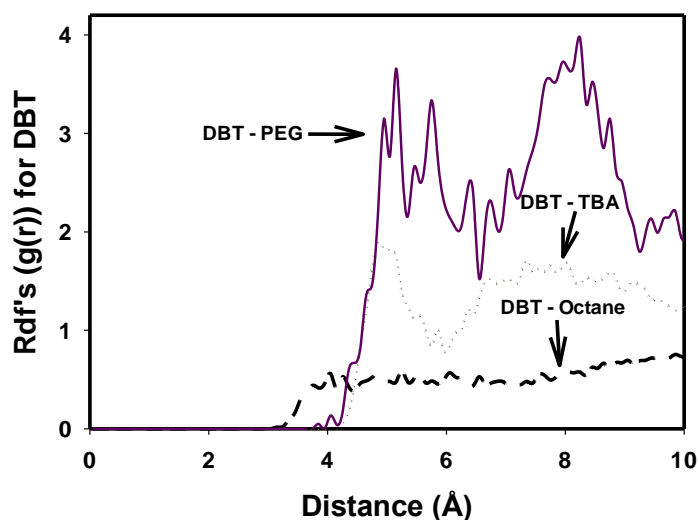


Figure 4.10. Rdfs for DBT with octane, TBA and PEG for the system 7.

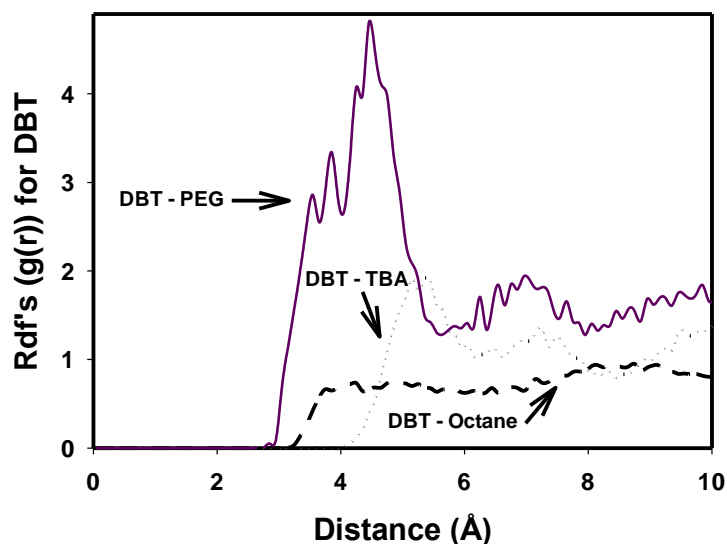


Figure 4.11. Rdfs for DBT with octane, TBAC and PEG at the system 8.

#### 4.3.2 Effect of temperature on the extraction process

The following analysis was completed in order to observe how increase of temperature may affect the desulfurization process. Therefore, system 4 was chosen for the study and the simulation was performed at 60 °C and 100 °C. The results are summarized in the table below:

Table 4.1. The energy profile for system 4 at 25°C, 60°C and 100°C.

<b>Interactions:</b>	<b>25 °C</b>	<b>60°C</b>	<b>100 °C</b>
<b>Octane-DBT (kJ/mol)</b>	-75.7	-59.7	- 93.6
<b>DES – DBT (kJ/mol)</b>	-157	-192	-99.7

The obtained results interestingly show that the desulfurization was achieved, as the interaction energies between DBT and DES in all cases is higher than for DBT and octane. Even though system simulated at 60 °C has higher interaction value for DES – DBT rather than system performed at 25 °C it can be seen that this difference is insignificant, and it proves that deep eutectic solvents can be effective at the room temperature resulting in the less energy consuming process. Moreover, it can be noticed that at 100 °C the interaction between DBT and octane increases, while interaction between DES and DBT decreases, and according to Li et al. this happens because of an exothermic reaction which takes place between DES and DBT at a certain high temperature [31].

### **4.3.3 Varying the type of thiophenes**

As a literature review showed the nature of thiophenic compound may affect the extraction efficiency. For example, Jiang et al. in their research tried to vary different sulfur compound such as dibenzothiophene, benzothiophene (BT), 4,6-dimethyldibenzothiophene (4,6-DMDBT) and mercaptan (RSH) in model oil to find out how the extraction efficiency was changed. According to their study the efficiency was shown in the following path: DBT > BT > 4,6-DMDBT > RSH, where DBT was the easiest extracted compound. One of the reasons for such outcome is that RSH has the lowest electron density because of the lack of delocalized  $\pi$  electrons. While 4,6-DMDBT was removed with low efficiency

because of the steric hindrance occurred between two methyl groups. Also, DBT has higher extraction activity in comparison with BT due to the higher number of aromatic rings which increases the interaction energy and finally, the alkyl group of 4,6-DMDBT leads to lower removal efficiency [30].

In another work by Li et al. (2016), the authors selected thiophene (TS), BT and DBT as representative substrates for desulfurization process. The extractive activity for each compound presented in the Figure 4.12. From this figure it is not clear which thiophenic compound has lower removal efficiency because it also depends on the type of DES which was used in the process [28].

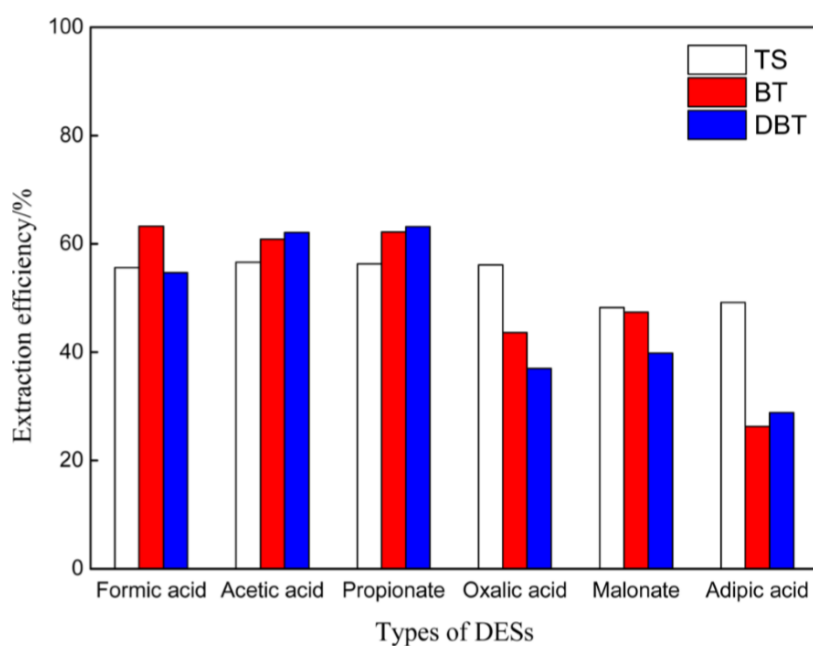


Figure 4.12 The extraction efficiency for sulfur compounds completed by various DES [28].



Therefore in this study TBAC:PEG:FeCl<sub>3</sub> was applied for removal of different sulfur substrates such as DBT, BT, TS to analyze how efficiency will be varied.

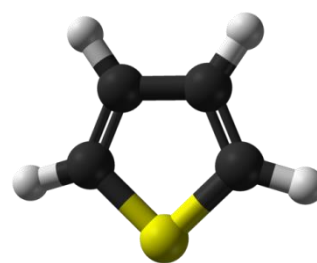
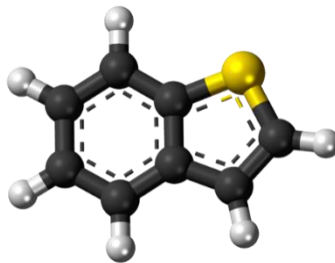
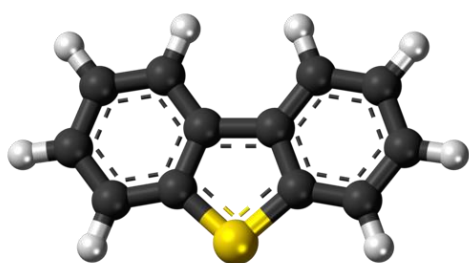


Figure 4. 13 DBT molecule [43]    Figure 4.14. BT molecule [44]    Figure 4.15. TS molecule [45]

In order to compare the results, we introduce a new variable R, a ratio between interaction energy of DES-thiophenes and octane-thiophenes (See table 4.2). As it can be seen from the table interaction forces between DBT and octane are the strongest, however, at the same time it has the highest DES – thiophenes interaction resulting in overall extraction ratio 2.07. BT molecule showed low interaction with octane and high with DES which came to the highest extraction ratio (2.64). Finally, the thiophene compound had the lowest interaction with octane but also with the solvents and thus, the extraction ratio was calculated to be the lowest ~1.57.

Table 2.2. The extraction efficiency for different thiophenes.

<b>Pair</b> <b>thiophenes</b>	<b>DBT</b>	<b>BT</b>	<b>TS</b>
<b>Octane-thiophenes (kJ/mol)</b>	-75.8	-47.1	-44.8
<b>DES-thiophenes (kJ/mol)</b>	-157	-125	-70.3
<b>Ratio (R)</b>	2.07	2.64	1.57

Even though the results show that all sulfur compounds can be removed from the fuel, still there is a huge difference in ratios BT > DBT > TS. The possible reason

for such trend is that TS among all sulfur compounds has the lowest electron cloud density resulting in the lowest extraction efficiency. While DBT molecule in spite of the highest electron density has large steric hindrance, which leads to lower extraction activity than for BT [28].

#### **4.4 Effect of DES constituent on the extraction process**

Different parameters such as molar ratio between DES compounds, type of hydrogen bond donor and acceptor may affect the extraction activity of thiophenic compounds. To investigate how each component contributes to desulfurization process, system consisting of TBAC:PEG (systems 11 & 12) and TBAC:FeCl<sub>3</sub> (systems 13 & 14) were simulated and analyzed.

##### **4.4.1 TBAC:PEG**

Earlier in 2013, Li et al. observed that TBAC:PEG mixtures can also form DES, and be used for fuel desulfurization. Their work showed 82.83% of sulfur removal efficiency after the first cycle which is lower than if it is with addition of ferric chloride (89.53%) [28]. From the figure below it can be seen that authors varied the molar ratios and the compounds inside the DES resulting for TBAC:PEG (1:2) being the most efficient.

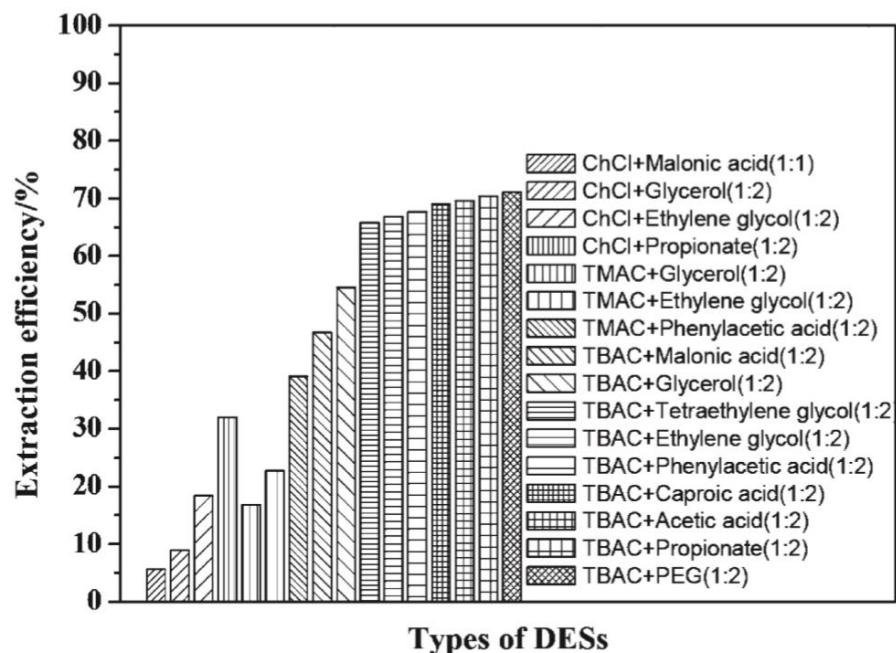


Figure 4.16. Different DES and their efficiencies as reported by Li et al. [28].

Therefore, TBAC:PEG with 1:2 molar ratio which was taken from the literature was simulated (system 11). Also, the molecular content was re-calculated keeping a mass fraction between DES and model oil 1:1. The operation conditions were the same as for the system 4 (25<sup>0</sup>C and 1 bar).

The interaction energy between DES and DBT in the system 4 is -157 kJ/mol, while for the system 11 is -147 kJ/mol (Table.3) which gives 7% difference and it is a reasonable explanation for the efficiency variance for TBAC:PEG:FeCl<sub>3</sub> and TBAC:PEG.

Also, as an experiment it was decided to run additional system 12, where FeCl<sub>3</sub> was simply removed from the mixture to keep the same numbers of molecules for TBAC

(400) and PEG (100). As a result the interaction energy between octane and DBT was higher than for DES-DBT which means that solvent was not able to extract the sulfur compounds (Table.3).

Table 4.3. Comparison of systems 11 and 12.

<b>Interactions:</b>	<b>System 11</b>	<b>System 12</b>
<b>Octane-DBT (kJ/mol)</b>	-88.9	-128
<b>DES – DBT (kJ/mol)</b>	-147	-114
<b>Ratio</b>	1.65	0.89

Summing up the obtained results it can be said that even a low amount of  $\text{FeCl}_3$  can affect the process. Yin et al. in 2016 proposed in their article that acidity of the system plays a key role for desulfurization efficiency [46]. Thus, the possible explanation for this phenomenon is that addition of  $\text{FeCl}_3$  which is a Lewis acid can affect the acidity of the DES solution and consequently, the efficiency of the process.

#### 4.4.2 TBAC: $\text{FeCl}_3$

The next two systems, which was simulated, excluded PEG from the desulfurization process. Taking into account that no articles were found where TBAC: $\text{FeCl}_3$  was used as a DES, the molar ratio between those components was chosen to be as a theoretical guess 2:1 based on the paper written by Gano et al. in 2014 where tetra-n-butyl phosphonium bromide was used as a quaternary salt and with combination of  $\text{FeCl}_3$  [47]. As a result system 13 was created with 366 molecules of TBA, 915

molecules of Cl and 183 molecules of FeCl<sub>3</sub>, keeping the mass ratio between model oil and DES 1:1.

In another case, to compare with our base system, numbers of atoms for TBA (400), Fe (5) and Cl (415) were used in the system 14. Both results of interaction energies are summarized in the table below:

Table 4.4. Interaction energies for systems 13 and 14.

<b>Interactions:</b>	<b>System 13</b>	<b>System 14</b>
<b>Octane-DBT (kJ/mol)</b>	-98.4	-70.8
<b>DES – DBT (kJ/mol)</b>	-119	-178
<b>Ratio (R)</b>	1.21	2.51

Although the mass ratio mass changed and no specific calculations were done the extraction ratio for system 14 was doubled in comparison with system 13 meaning that the theoretical assumption which was done before is incorrect.

Taking into account that obtained results for system 14 seem to be even better than for system 4 both systems were compared in Figure 4.17 where the interactions between DES-octane and DBT-octane are summarized.

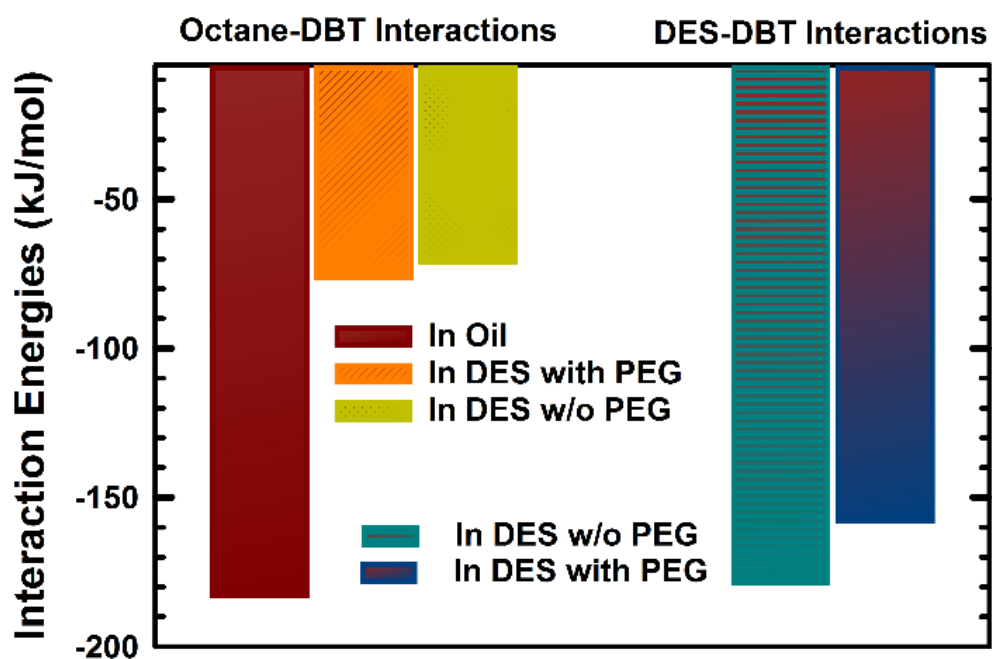


Figure 4.17. Interaction energies for systems 4 and 14.

It can be seen that DES without PEG can be not only be effective in the desulfurization process but it also has a comparative efficiency.

## Chapter 5 - Conclusion and future work

This research was aimed to understand the molecular interaction occurring in the metallic deep eutectic solvent and the desulfurization process. The results with TBAC:PEG:FeCl<sub>3</sub> at 4:1:0.05 molar ratio at under 25 °C and 1 bar show that each individual chemical compound initially has a very strong interaction energy, however, after mixing let to a decrease in the total interaction energy. Moreover, to check its sulfur extraction abilities DES was mixed with model fuel (n-octane) with 2000 ppm DBT concentration and it was observed that all sulfur molecules were captured by solvents. Additionally, different parameters such as temperature, sulfur concentration, composition of model oil and DES were varied to observe the behavior of desulfurization process. And as a result, it can be said that TBAC:PEG:FeCl<sub>3</sub> was effective at desulfurization of diesel with even high level of sulfur concentration and also it could remove other thiophenic compounds (BT and TS). Moreover, it was proved that DES is more effective at room temperature, while at high temperatures interaction between solvents and sulfur becomes weaker. Finally, DES composition was varied by removing PEG and FeCl<sub>3</sub> from the system and the results showed that TBAC:FeCl<sub>3</sub> can have even higher extraction abilities than TBAC:PEG:FeCl<sub>3</sub>.

Although use of molecular dynamics simulation allowed us to observe the mechanism of DES formation and desulfurization process, there are some aspects left undiscovered which requires additional study. One of them could be variation of model oil composition. In this work n-octane was used as a fuel compound with single sulfur compound (DBT). So as an option, n-octane can be mixed other hydrocarbons such as decane and dodecane to better mimic the actual fuel. Additionally to that, DBT, BT and TS can be added simultaneously to the mixture. Chemistry of the desulfurization process must further be studied, as Li et al. did not give answers why exactly  $\text{FeCl}_3$  has better performance in extraction in comparison with other metallic salts, which were also transit metals from the same period. And also taking into account that  $\text{FeCl}_3$  did not interact with sulfur compounds it somehow changed the properties of mixture so that extract efficiency increased significantly. Our assumption was that this salt may affect acidity by making a reference to the paper written by Yin et al. in 2016.

Finally, this paper covers only simulation, therefore if it is combined with an experimental part it might give justified results. Especially, in the part where composition of DES was varied to check if  $\text{TBAC}:\text{FeCl}_3$  is really more effective than  $\text{TBAC}:\text{PEG}:\text{FeCl}_3$ . Furthermore, the recovery of the DES by using anti-solvent needs to be analyzed.



## Reference list

1. Hao, L., Wang, M., Shan, W., Deng, C., Ren, W., Shi, Z. and Lu, H., *L-proline-based deep eutectic solvents (DESs) for deep catalytic oxidative desulfurization (ODS) of diesel*. . Journal of Hazardous materials 2017. **339**: p. 216-222.
2. Zaid, H.F.M., Kait, C. F. and Mutalib, M. I. A., *Extractive deep desulfurization of diesel using choline chloride-glycerol eutectic-based ionic liquids as a green solvent*. . Fuel, 2017. **197**: p. 10-17.
3. Li, J., Xiao, H., Tang, X. and Zhou, M., *Green Carboxylic Acid-Based Deep Eutectic Solvents as Solvents for Extractive Desulfurization*. . Energy fuels, 2016. **30**: p. 5411–5418.
4. Warrag, S.E.E., Peters, and Kroon, M. C. , *Deep eutectic solvents for highly efficient separations in oil and gas industries*. Current Opinion in Green and Sustainable Chemistry 2017. **5**: p. 55–60.
5. Hayyan, M., Alakrach, A. M., Hayyan, A., Hashim, M. A., and Hizaddin, H. F. , *Superoxide Ion as Oxidative Desulfurizing Agent for Aromatic Sulfur Compounds in Ionic Liquid Media*. ACS Sustainable Chem. Eng. , 2017. **5**: p. 1854–1863.
6. Bernasconi, R., Panzeri, G., Accogli, A., Liberale, F., Nobili, L. and Magagnin, L., *Electrodeposition from Deep Eutectic Solvents*. , in *Progress and development in ionic liquids*. , S. Handy, Editor 2017, Intech
7. Li, C., Zhang, J., Li, Z., Yin, J., Cui, Y., Liua, Y. and Yanga, G. , *Extraction desulfurization of fuels with 'metal ions' based deep eutectic solvents (MDESs)*. . Green Chem. , 2016. **18**: p. 3789-3795.
8. Xu, P., Zheng, G., Zong, M., Li, N. and Lou, W., *Recent progress on deep eutectic solvents in biocatalysis*. . Bioresour Bioprocess, 2017. **4**(1).
9. Abbott, A.P., Boothby, D., Capper, G., Davies, D. L., and Rasheed, R. K. , *Deep Eutectic Solvents Formed between Choline Chloride and Carboxylic Acids: Versatile Alternatives to Ionic Liquids*. . American Chemical Society 2004. **126**(29): p. 9142–9147.
10. Smith, M.L., Abbott, A.P., and Ryder, K. S., *Deep Eutectic Solvents (DESs) and Their Applications*. Chem. Rev., 2014. **114**(21): p. 11060–11082.
11. García, G., Aparicio, S., Ullah, R. and Atilhan, M., *Deep Eutectic Solvents: Physicochemical Properties and Gas Separation Applications*. Energy & Fuels 2015. **29**(4): p. 2616-2644.
12. Stefanovic, R., Ludwig, M., Webber, G.B., Atkin, R. and Page, A. J., *Nanostructure, hydrogen bonding and rheology in choline chloride deep eutectic solvents as a function of the hydrogen bond donor*. Phys. Chem. Chem. Phys., 2017. **19**: p. 3297 - 3306.
13. Taysun, M.B., Sert, E. and Atalay, F.S., *Effect of Hydrogen Bond Donor on the Physical Properties of Benzyltriethylammonium Chloride Based Deep Eutectic Solvents and Their Usage in 2-Ethyl-Hexyl Acetate Synthesis as a Catalyst*. J. Chem. Eng. Data, 2017. **62**(4): p. 1173–1181.
14. Abbott, A.P., J. C. Barron, K. S. Ryder, and D. Wilson. , . *Eutectic-Based Ionic Liquids with Metal-Containing Anions and Cations*. Chemistry – A European Journal 2007. **13**: p. 6495-6501.
15. Mjalli, F., and Shah, D., *Simulation Based Insight into Solvation Properties of Ferric Chloride Based Eutectic Solvent*. Chemical Engineering Transactions, 2015. **43**: p. 1843-1848.

16. Banisharif, F., Dehghani, M. R., Capel-Sánchez, M., and Campos-Martin, J.M. , *Desulfurization of Fuel by Extraction and Catalytic Oxidation Using a Vanadium Substituted Dawson-Type Emulsion Catalyst*. Ind. Eng. Chem. Res. , 2017. **56**: p. 3839–3852.
17. Phadtare, S.B.a.S., G.S., *Halogenation reactions in biodegradable solvent: Efficient bromination of substituted 1-aminoanthra-9, 10-quinone in deep eutectic solvent (choline chloride: urea)*. Green Chemistry 2010. **12**(3): p. 458-462.
18. Singh, B., Lobo, H. and Shankarling, G., *Selective N-alkylation of aromatic primary amines catalyzed by bio-catalyst or deep eutectic solvent*. Catalysis letters 2011. **141**(1): p. 178-182.
19. Raul Calderon Morales, V.T., Paul R. Jenkins,\* David L. Davies and Andrew P. Abbott, *The regiospecific Fischer indole reaction in choline chloride·2ZnCl<sub>2</sub> with product isolation by direct sublimation from the ionic liquid*. Chemical Communications, 2004(2): p. 158–159.
20. Sarmad, S., Mickkola, J. P., and Ji, X. , *Carbon dioxide capture with Ionic liquids and deep eutectic solvents: a new generation of sorbents*. . ChemSusChem, 2017. **10**: p. 324-352.
21. Zulkurnai, N.Z., Md. Ali, U. F., Ibrahim, N., and Abdul Manan, N.S., *Carbon Dioxide (CO<sub>2</sub>) Adsorption by Activated Carbon Functionalized with Deep Eutectic Solvent (DES)*. Materials Science and Engineering 206 012001, 2016.
22. Zhu, A., Jiang, T., Han, B., Zhang, J., Xie, Y. and Ma, X., *Supported choline chloride/urea as a heterogeneous catalyst for chemical fixation of carbon dioxide to cyclic carbonates*. Green Chem., 2007: p. 169-172.
23. Zubeir, L.F., Lacroix, M.H. and Kroon, M.C., *The low transition temperature mixture 'lactic acid+ tetramethylammonium chloride (2:1)' as novel CO<sub>2</sub> capture solvent*. . J. Phys. Chem. B, 2014. **118**(49): p. 14429–14441.
24. Warrag, S., Peters, C. and Kroon, M. , *Deep eutectic solvents for highly efficient separation in oil and gas industries*. Current Opinion in Green and Sustainable Chemistry 2017. **5**: p. 55–60.
25. Rodriguez, N.R., Requejo, P. F. and Kroon, M. C. , *Aliphatic – aromatic separation using deep eutectic solvents as extracting agents*. Ind. Eng. Chem. Res. , 2015. **54**(45): p. 11404-11412.
26. Gonzales, S., Francisco, M., Jimeno, G., De Dios S. and Kroon, M., *Liquid-liquid equilibrium data for the systems (LTTM + benzene + hexane) and (LTTM + ethyl acetate + hexane) at different temperatures and atmospheric pressure*. Fluid Phase Equilibria, 2013. **360**: p. 54-62.
27. Abbott, A.P., Cullis, P., M., Gibson, M.J., Harris, R.C. and Raven E. , *Extraction of glycerol from biodiesel into a eutectic based ionic liquid*. Green Chem., 2007. **9**(8): p. 868.
28. Li, C., Li, D., Zou, S., Li, Z., Yin, J., Wang, A., Cui, Y., Yao, Z. and Zhao, Q. , *Extraction desulfurization process of fuels with ammonium-based deep eutectic solvents*. Green Chemistry, 2013. **15**: p. 2793–2799
29. Tang, X., Zhang, Y., Li, J., Zhu, Y., Qing, D. and Deng, Y, *Deep Extractive Desulfurization with Arenium Ion Deep Eutectic Solvents*. Ind. Eng. Chem. Res. , 2015. **54**: p. 4625–4632.
30. Jiang, W., Li, H., Wang, C., Liu, W., Guo, T., Liu, H., Zhu, W. and Li, H. , *Synthesis of Ionic-Liquid-Based Deep Eutectic Solvents for Extractive Desulfurization of Fuel*. Energy fuels, 2016. **30**: p. 8164–8170.

31. Li, C., Zhang, J., Li, Z., Yin, J., Cui, Y., Liu, Y. and Yang, G., *Extraction desulfurization of fuels with 'metal ions' based deep eutectic solvents (MDESs)*. Green Chemistry, 2016. **18**: p. 3789–3795
32. Li, J., Xiao, H., Tang, X., and Zhou, M. , *Green Carboxylic Acid-Based Deep Eutectic Solvents as Solvents for Extractive Desulfurization*. Energy fuels, 2016. **30**: p. 5411–5418.
33. Shu, C., & Sun, T., *Extractive desulfurization of gasoline with tetrabutylammonium chloride-based deep eutectic solvents*. SEPARATION SCIENCE AND TECHNOLOGY, 2017. **51**(8): p. 1336–1343
34. Jiang, W., Dong, L., Guo, T., Li, H., Yin, S. and Zhu, W. , *Biodegradable choline-like deep eutectic solvents for extractive desulfurization of fuel*. Chemical Engineering and Processing 2017. **115**: p. 34-38.
35. Al Ani, Z.A., Al Wahaibi, T., Mjalli, F.S., Al Hashmi, A., and Abu-Jdayil, B., *Flow of deep eutectic solvent-simulated fuel in circular channels: Part II—Extraction of dibenzothiophene*. Chemical Engineering Research and Design 2017. **119**: p. 294-300.
36. Rahma, W., Mjalli, F. and Al-Wahaibi, T. , *Polymeric-based deep eutectic solvents for effective extractive desulfurization of liquid fuel at ambient conditions*. Chemical Engineering Research and Design, 2017. **120**: p. 271-283.
37. Griebel, M., Knapek, S. and Zumbusch, G., *Numerical Simulation in Molecular Dynamics: Numerics, Algorithms, Parallelization, Applications*. Vol. 5. 2007: Springer Science & Business Media.
38. Allen, M.P., *Introduction to Molecular Dynamics Simulation*, 2004, John von Neumann Institute for Computing: Computational Soft Matter: From Synthetic Polymers to Proteins. p. 1-28.
39. Koziara, K., Stroet, M., Malde, A. and Mark, A., *Testing and validation of the Automated Topology Builder (ATB) version 2.0: prediction of hydration free enthalpies*. Journal of Computer-Aided Molecular Design 2014. **28**(3): p. 221-233.
40. Lin, W., Welsh, W. J., and Harris, W. R. , *Molecular mechanics studies of model iron(III) transferrin complexes in vacuo and in aqueous solution*. . Inorg. Chem. , 1994. **33**: p. 884–890.
41. Schmid, N., Eichenberger, A., Choutko, A., Riniker, S., Winger, M., Mark, A. and van Gunsteren, W., *Definition and testing of the GROMOS force-field versions 54A7 and 54B7*. European Biophysics Journal 2011. **40**(7): p. 843-856.
42. Chemistry, R.S.o., *ChemSpider*.
43. Wikipedia, ed. *Ball-and-stick model of the benzothiophene molecule, a sulfur heterocycle and a simple aromatic ring*. Discovery Studio Visualizer., ed. Benzothiophene-3D-balls-2.png2011.
44. Wikipedia *Ball-and-stick model of the dibenzothiophene molecule*. Discovery Studio Visualizer, 2011.
45. Mills, B. *Ball-and-stick model*. Accelrys DS Visualizer., 2009.
46. Yin, J., Wang, J., Li, Z., Li, D., Yang, G., Cui, Y., Wang, A., and Li, C. , *Deep desulfurization of fuels based on an oxidation extraction process with acidic deep eutectic solvents*. Green Chemistry, 2015. **17**(9): p. 4552–4559
47. Gano, Z., Mjalli, F. S., Al-Wahaibi, T., Al-Wahaibi, Y. and Al Nashef, I.N. , *Extractive desulfurization of liquid fuel with FeCl<sub>3</sub>-based deep eutectic solvents: Experimental design and optimization by central-composite design*. Chemical Engineering and Processing, 2015. **93**: p. 10-20.

# Appendix A

The results generated at 298 K and 1 bar which are shown below, indicate that oil and DES are immiscible.

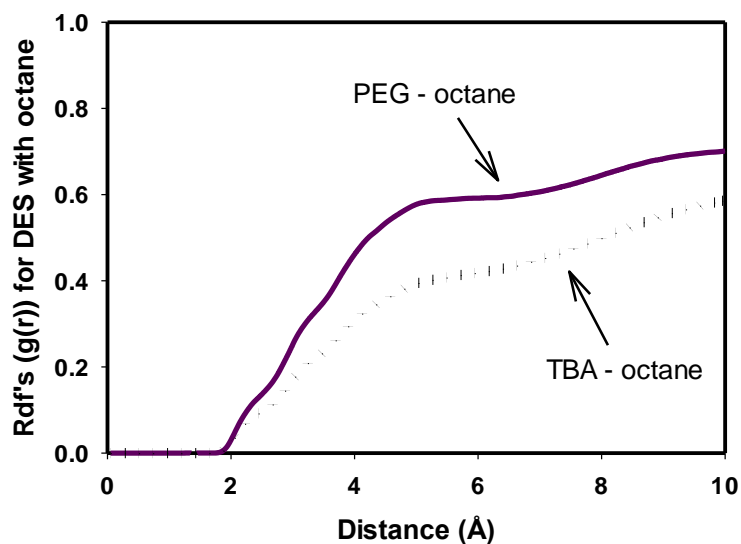


Figure A1. Rdfs between PEG-octane and TBA-octane indicating low peak values (less than 0.) show that the interaction between DES and octane is weak.

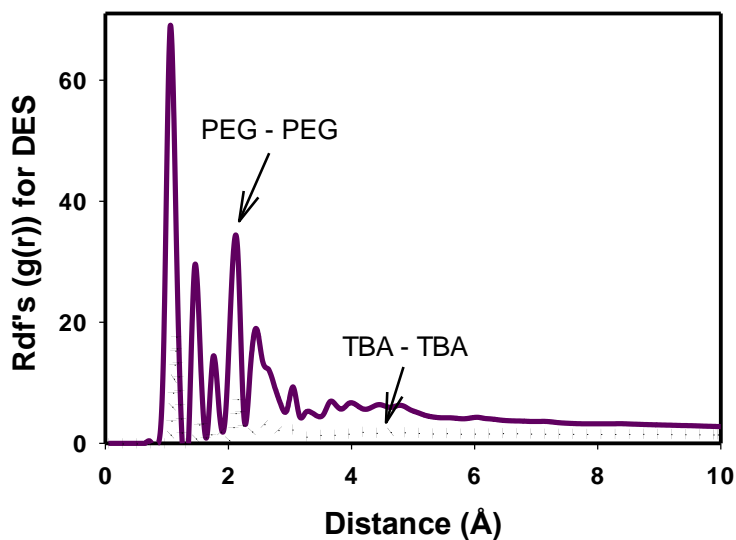


Figure A2. Rdfs for PEG-PEG and TBA-TBA with peak values 70 and 18 respectively, indicate that interaction inside DES's molecules is strong even in the presence of octane.

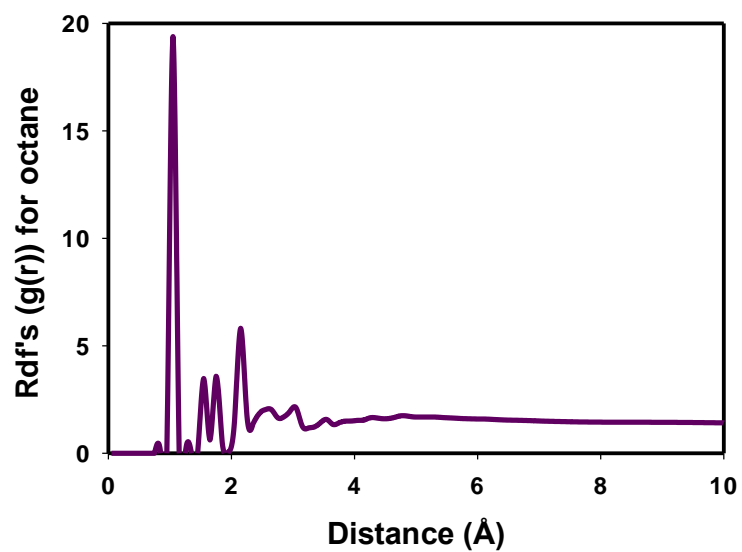


Figure A3. Rdf for octane-octane with peak value 19 results in high interaction between octane molecules in fuel in the presence of DES.

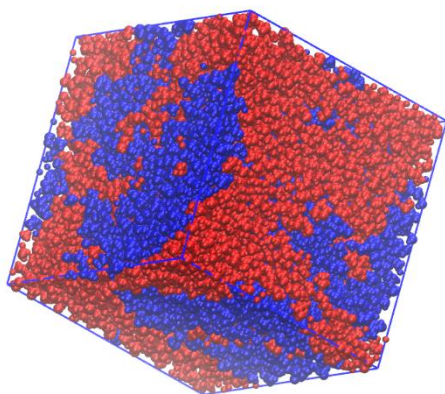


Figure A4. A box with octane (red) and DES (blue) at 298 K and 1 bar. With addition of plots above it summarizes that DES and octane are not mixable.